Tertiary Butyl Nitrite Triggered Nitration of Phenols: Solvent- and Structure-Dependent Kinetic Study

M. SATISH KUMAR,[1] K. C. RAJANNA,[1] M. VENKATESWARLU,[1] K. LAKSHMAN RAO[2]

[1] *Department of Chemistry, Osmania University, Hyderabad, 500 007, India*

[2] *Department of Statistics, Osmania University, Hyderabad, 500 007, India*

Received 9 July 2015; revised 10 December 2015; accepted 14 December 2015

DOI 10.1002/kin.20979

ABSTRACT: Nitration of phenols with tertiary butyl nitrite (TBN) obeyed second-order kinetics with a first-order dependence on [TBN] and [phenol] under acid-free conditions. Reaction rates were significantly altered by a change in the dielectric constant and other physical properties of solvent. The rate of nitration increased with an increase in temperature (303–323 K) in different solvent media (acetonitrile, dichloroethane, CCl_4, dimethyl formamide (DMF), and toluene). The rates of nitration (log k) could not fit into either Amis or Kirkwood plots [log k' vs. (1/D) or [(D − 1)/(2D + 1)], but the trends were better explained by the basic form of multivariate linear solvent energy relationships (MLSER) suggested by the Koppel and Palm approach on the one hand and the Kamlet and Taft approach on the other hand. These observations probably substantiate that cumulative contributions of basic solvent parameters (equilibrium as well as frictional solvent effects) and solvent–solute interactions for solvation of transition state during nitration of phenols. Reaction rates accelerated with the introduction of electron-donating groups and retarded with electron-withdrawing groups. Accordingly, the reactivity of structurally different phenols was found to follow the following sequence: p-OH > p-MeO > p-Me > H > m-Me > p-Cl > p-Br > m-Cl > p-NO_2 > m-OH. The results are interpreted by Hammett's theory of linear free energy relationship. The reaction constant (Hammett's ρ) is a measure of the sensitivity of the reaction toward the electronic effects of the substituent. The rho (ρ) values obtained from the present experiments are fairly large negative values ($\rho < 0$), indicating attack of an electrophile on the aromatic ring. An increase in temperature

---

Correspondence to: K. C. Rajanna; e-mail: kcrajannaou@yahoo.com.

Supporting Information is available in the online issue at www.wileyonlinelibrary.com.

decreases the reaction constant (ρ) values. According to Exner, ρ values for a given reaction are influenced by the temperature according to the following relation: $\rho = A\,[1 - \beta/T]$. Obtained "isokinetic temperature (β)" values are in the range of 225–290. These values are far below the experimental temperature range (303–323 K), indicating that the entropy factors are probably more important in controlling the reaction. This point can be seen from the negative entropy values and linearity of multiple linear regression analysis (MLRA). Furthermore, in the present study, rate constants for TBN nitration of ortho-substituted phenols could not fit into Taft's plots of $\log(k/k_{CH3})$ versus σ^* or, E_s or combined Taft's relationship. However, Charton's MLRA of the log k with polar, resonance, steric, hydrophobicity, and molar refractivity showing a very good linear relationship was obtained. It is of interest to note that when log k_{exp} values are correlated with log k_{cal} a perfect linearity is obtained with a correlation coefficient of unity, indicating the consonance between experimental and calculated rate constants in the present work. © 2016 Wiley Periodicals, Inc. Int J Chem Kinet 48: 171–196, 2016

INTRODUCTION

Nitration is one of the most important classes of chemical processes for the introduction of a nitro group into an organic chemical compound. Nitration reaction exhibited a broad spectrum of industrial applications. A large number of nitroaromatic compounds are widely used as solvents, explosives, pharmaceuticals, and also as chemical intermediates and precursors in the manufacturing of synthetic dyestuffs and other chemicals [1–3]. In the classical nitration method, "acid mixture (nitric acid and sulfuric acid)" is used as a nitrating regent to produce the nitronium ion (NO_2^+), which is the active species for nitration. The existence of the nitronium ion has been determined spectroscopically with a line at 1400 cm^{-1} in the Raman spectrum, which indicates the presence of a species that is both linear and triatomic [4]. This active ingredient has been isolated in the case of nitronium tetrafluoroborate, [5], which also affects nitration without the need for the mixed acid. Hughes et al. [6] stated that Martinsen (1904) was the first person to obtain a definite kinetic order for the nitration of aromatic substances in sulfuric acid medium. The reaction exhibited clear second-order kinetics in this medium. In this paper, Benford and Ingold obtained the first well-defined kinetic results in any solvent other than sulfuric acid. With nitromethane as solvent, and nitric acid in constant excess; they demonstrated zero-order kinetics in [HNO_3]. However, this insensitiveness of the rate to the concentration and nature of the aromatic compound applied only to relatively reactive compounds, such as benzene and toluene. Kinetics of aromatic nitration studied by Halberstadt et al. in the same year [7] lead to the conclusion that the nitracidium ($H_2NO_3^+$) and nitronium ions (NO_2^+) are successively formed during nitration by nitric acid, but that only the nitronium ion (NO_2^+) is effective for nitration in anhydrous or nearly anhydrous acid. This note offers evidence for the effectiveness, under other conditions, of the nitracidium ion ($H_2NO_3^+$) as a nitrating agent. In later years, Kecki [8] gave a detailed account on the role of acidity in the nitration of aromatic compound from detailed kinetic studies. The colorimetric method was used for investigation of the nitration kinetics in the following solutions: ($HNO_3 + H_2O$), ($HNO_3 + CH_3COOH + H_2O$), ($HNO_3 + H_2SO_4 + H_2O$), ($HNO_3 + HClO_4 + H_2O$). Mechanisms of nitration of aromatic compounds based on a system of protolytic equilibria are proposed. The advent of miniaturized devices has paved the way for new opportunities to reconsider the conventional approach for exothermic and selectivity sensitive nitration reactions. In a recent review in the field of continuous flow nitration, Kulkarni [9] highlighted four different approaches for flow nitration with microreactors highlighted their advantages, limitations ,and applicability of the information toward scale-up. On the other hand, the classical method of nitration of organic compounds [using the acid mixture (HNO_3 and H_2SO_4)] has been proved hazardous, highly toxic, and corrosive. These shortcomings and limitations lead to design and execute of mild methods of nitration of aromatic compounds [10–22].

Tertiary butyl nitrite (TBN) is an alkyl ester of nitrous acid (R-ONO), where the alkyl group (R) represents the *t*-butyl moiety. It is distinct from a nitro compound (R-NO_2). In a recent publication, Koley et al reported a nitration method using TBN [23] under acid-free conditions, compatible with tyrosine-containing peptides on solid support in the synthesis of fluorogenic substrates for characterization of proteases. Kilpatrick and Arns demonstrated TBN as an effective reagent for the selective nitration of aryl sulfonamides [24]. Encouraged by the features reported in this paper, we have recently reported the nitrodecarboxylation of α,β-unsaturated acids for the synthesis of β-nitrostyrenes under acid-free conditions by TBN and extended the methodology for nitration of aromatic compounds. The reactions were also studied under nonconventional methods such as microwave-assisted (solvent-free) and sonicated (solution-phase) conditions [25]. Even though, ample literature is available on the kinetics of nitration in the presence of "acid mixture" [5–9] since 1904, not much focus has been paid on the kinetics of nitration of organic compounds under acid-free conditions. In this work, we have taken up a detailed colorimetric kinetic study of nitration of phenols using TBN in different solvents to gain an insight into mechanistic aspects. Nevertheless, recently we have reported kinetic and mechanistic study of polyethylene glycols triggered decarboxylative nitration of α,β-unsaturated aromatic acids by ceric ammonium nitrate and (Fe(III)-bipy)chelate (where bipy = 2,2′-bipyridyl ligand) in MeCN medium [26].

EXPERIMENTAL

General

Chemicals purchased from Aldrich (India), Merck (India), Loba (India), or Fluka (India) were of reagent grade. The solvents of this study were fractionally distilled before use. Products of the reactions were characterized by spectroscopic methods and physical data such as melting/boiling points. Melting points were recorded on a Buchi B-545 capillary melting point apparatus and were uncorrected. Infrared (IR) spectra were recorded on a Perkin Elmer FT-IR spectrometer. ^{1}H NMR spectra were recorded at a Varian VNMRS-300 MHz spectrometer. Chemical shifts are reported as values in ppm relative to $CHCl_3$ (7.26), and TMS was used as an internal standard. Mass spectra were recorded on a ZAB-HS mass spectrometer using ESI ionization.

Kinetic Method of Following the Reaction

A flask containing a known amount of TBN in a suitable solvent (generally acetonitrile solvent) and another flask containing the substrate (phenol) along with other additives (if any) were clamped in a thermostat (constant temperature bath) at a desired temperature. By mixing a requisite amount of TBN with the other contents of the reaction vessel, the reaction was initiated and mixed the contents thoroughly. Black-coated flasks from outside were used to prevent photochemical effects. Aliquots of the reaction mixture were withdrawn into a cuvette and placed in the cell compartment of the laboratory visible spectrophotometer. The cell compartment was provided with an inlet and an outlet for circulation of thermostatic liquid at a desired temperature. The TBN content could be estimated from the previously constructed calibration curve, showing absorbance (A) versus [TBN] at 430 nm. Absorbance values were in agreement with each other with an accuracy of ±3% error.

RESULTS AND DISCUSSION

Determination of the Order of Reaction

To determine **"**order of the reaction," we have used the graphical method of approach based on the integrated rate expressions of second-order and first-order kinetics, according to standard procedures. If A_t is absorbance of nitrate species produced during the course of reaction at a given time, A_∞ is the absorbance at infinite time (at the end of the reaction), and A_0 is the absorbance (if any) before the on-take of reaction, then $(A_\infty - A_t)$ is proportional to $(a - x)$ and $(A_\infty - A_0) = (a)$.

(i) Kinetic plots of $[1/(a - x)]$ or $(1/(A_\infty - A_t))$ versus time of this reaction with equal concentrations of $[\mathrm{TBN})]_0 = [\mathrm{S}]_0$ (under second-order conditions) have been found to be linear with a positive gradient and definite intercept on the ordinate (vertical axis) indicating overall second-order kinetics (as typical examples, Fig. 1, and 2 are given), according to the following expression:

$$\frac{1}{(a-x)} = \frac{1}{(a)} + kt \tag{1}$$

(ii) Under the conditions, viz., [phenol] >> [TBN)], the plots of $\ln [(A_\infty - A_0)/(A_\infty - A_t)]$or $[\ln (a/(a - x)]$ versus. time were linear with a positive slope passing through origin according to the following equation:

$$\ln \frac{a}{(a-x)} = kt \tag{2}$$

This observation indicated first-order kinetics in [TBN)] in all the systems studied. The First-order rate constant (k') could be obtained from the slopes of these linear plots. Since the order with respect to [TBN] is already verified as one under pseudoconditions and overall order is second order, it is clear that order in [S] is also one. Similar observations were noticed when the reactions were studied in all the solvents used in this study (as typical examples Figs. 3 and 4 are shown).

Accordingly, in the present study, the rate law of TBN-mediated nitration of phenols could be represented by considering Scheme 1:

$$\mathrm{TBN} + \mathrm{Phenol} \rightarrow \mathrm{Products} \tag{3}$$

Time (min)	O.D (Absorbance)	$1/(A_{\infty}-A_{t})$
0	0.11	7.14286
5	0.11	7.14286
10	0.12	7.69231
15	0.12	7.69231
20	0.13	8.33333
25	0.13	8.33333
30	0.14	9.09091
35	0.14	9.09091
40	0.15	10
45	0.15	10
50	0.16	11.1111
55	0.16	11.1111
60	0.17	12.5

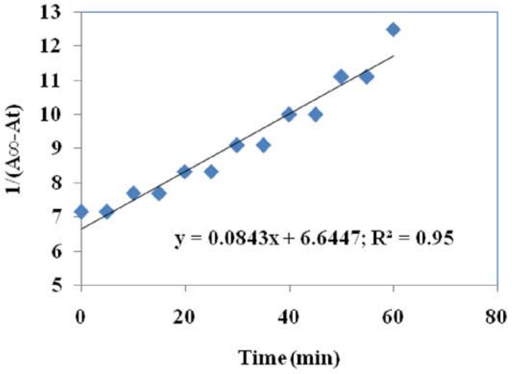

Figure 1 Plot of $[1/(A_{\infty} - A_t)]$ versus time (second-order plot). [*p*-Cresol] = 0.01 mol/dm^3; [TBN] = 0.01 mol/dm^3; solvent = MeCN; temperature = 303 K.

Time (min)	O.D (Absorbance)	$1/(A_{\infty}-A_{t})$
0	0.04	7.69231
5	0.07	10
10	0.1	14.2857
15	0.12	20
20	0.13	25
25	0.14	33.3333
30	0.15	50
60	0.16	100

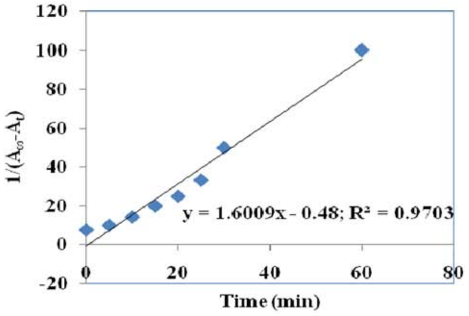

Figure 2 Plot of $[1/(A_{\infty} - A_t)]$ versus time (second-order plot). [*m*-Chloro phenol] = 0.01 mol/dm^3; [TBN] = 0.01 mol/dm^3; solvent = DCE; temperature = 303 K.

Time (min)	O.D (Absorbance)	$\ln[(A_{\infty}-A_{0})/(A_{\infty}-A_{t})]$
0	0.21	0
5	0.26	0.13005
10	0.31	0.27958
15	0.35	0.41774
20	0.39	0.57808
25	0.41	0.66905
30	0.43	0.76913
35	0.45	0.88036
40	0.46	0.94098
45	0.47	1.00552
50	0.49	1.14862
55	0.5	1.22867
60	0.51	1.31568

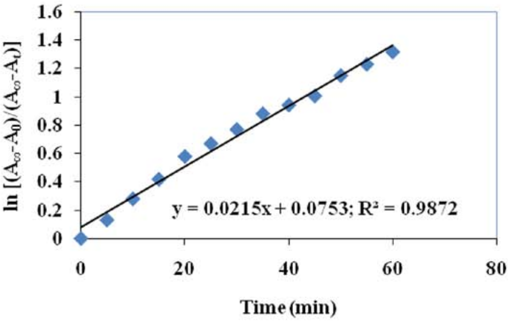

Figure 3 Plot of $\ln[(A_{\infty} - A_0)/(A_{\infty} - A_t)]$ versus time (first-order plot). [Phenol] = 0.10 mol/dm^3; [TBN] = 0.01 mol/dm^3; solvent = MeCN; temperature = 303 K.

Time	O.D	$\ln [(A_\infty\text{-}A_0)/(A_\infty\text{-}A_t)]$
0	0.1	0
5	0.11	0.105361
10	0.12	0.223144
15	0.13	0.356675
20	0.13	0.356675
25	0.14	0.510826
30	0.14	0.510826
35	0.14	0.510826
40	0.15	0.693147
45	0.15	0.693147
50	0.16	0.916291
55	0.16	0.916291
60	0.16	0.916291

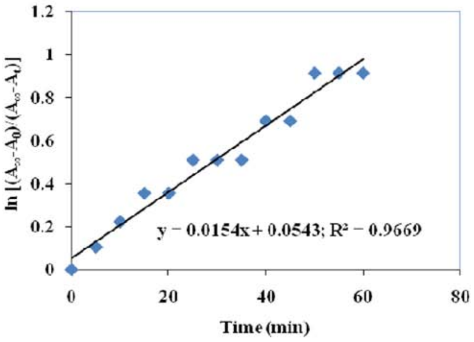

Figure 4 Plot of ln $[(A_\infty - A_0)/(A_\infty - A_t)]$ versus time (first-order plot). [*p*-Br Phenol] = 0.10 mol/dm^3; [TBN] = 0.01 mol/dm^3; solvent = MeCN; temperature = 303 K.

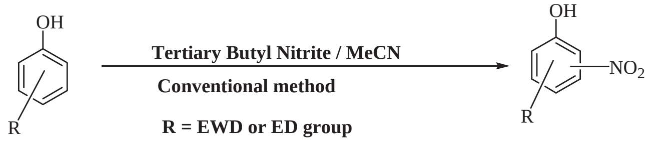

Scheme 1 Nitration of phenols under conventional conditions.

$$\text{Rate (V)} = (-\,\mathrm{d}[\text{TBN}]/\mathrm{d}t) = k_1[\text{TBN}][\text{S}] \qquad (4)$$

Product Analysis

To a solution of phenol (1 mmol) in acetonitrile was added TBN (1 mmol) and stirred for 1 hr. The progress of the reaction was monitored by TLC. After completion of the reaction, the reaction mixture was treated with 5% sodium thiosulfate (Hypo) solution. The organic layer was separated and dried over Na_2SO_4 and evaporated under vacuum. Column chromatography was used to purify crude product. A binary mixture of ethylacetate and hexane (3:7) was used as an eluent to get a pure product 4-nitro phenol as a yellow powder (mp 111–113°C) in 85% yield, IR(KBr) ($\nu_{\max}$ (cm^{-1})): 3331, 1614, 1592, 1500, 1346; 1H NMR (300 MHz, CDCl3): δ 9.95 (s 1H, OH), 6.95 (d 2H, J = 8 Hz), 8.15 (d 2H, J = 8 Hz); HRMS (EI) Calcd. M, 139.1086, Found: 139.0274

Spectral data of other Nitro phenols:

1. **4-Me 2-NO$_2$ Phenol**: ^{1}H NMR (300 MHz, $CDCl_3$): δ 10.42 (s, 1H, OH), 2.42 (s, 3H, Me), 7.32 (d, 1H, J = 8 Hz), 7.12 (d, 1H, J = 8 Hz), 7.92 (s, 1H); mp = 32–34°C; HRMS (EI) Calcd. M, 153.1351, Found: 153.0438.
2. **4-Cl 2-NO$_2$ Phenol**: ^{1}H NMR (300 MHz, $CDCl_3$): δ 10.54 (s, 1H, OH), 7.12 (d, 1H, J = 8 Hz), 7.82 (d, 1H, J = 8 Hz), 8.36 (s, 1H); mp = 88–90°C; HRMS (EI) Calcd. M, 173.5534, Found: 172.9894.
3. **4-Br 2-NO$_2$ Phenol**: ^{1}H NMR (300 MHz, $CDCl_3$): δ 10.45 (s, 1H, OH), 7.10 (d, 1H, J = 8 Hz), 7.72 (d, 1H, J = 8 Hz), 8.25 (s, 1H); mp = 92–96°C; HRMS (EI) Calcd. M, 218.0047, Found: 217.9358.
4. **2-NO$_2$ Benzene 1,4 diol**: ^{1}H NMR (300 MHz, $CDCl_3$): δ 10.26 (s, 2H, OH), 7.14 (d, 1H, J = 8.5 Hz), 6.92 (d, 1H, J = 8.5 Hz), 7.48 (s, 1H); bp = 306–308°C; HRMS (EI) Calcd. M, 155.1082, Found: 155.0226.
5. **4-OMe-NO$_2$ Phenol**: ^{1}H NMR (300 MHz, $CDCl_3$): δ 10.36 (s, 1H, OH), 3.85 (s, 3H, Me), 7.09 (d, 1H, J = 8 Hz), 7.22 (d, 1H, J = 8 Hz), 7.54 (s, 1H); mp = 82–84°C; HRMS (EI) Calcd. M, 169.1345, Found: 169.0382.
6. **2,4 Dinitro Phenol**: ^{1}H NMR (300 MHz, $CDCl_3$): δ 10.92 (s, 1H, OH), 7.26 (d, 1H, J = 8 Hz), 8.38 (d, 1H, J = 8 Hz), 9.02 (s, 1H); mp

= 107–109°C; HRMS (EI) Calcd. M, 184.1062, Found: 184.0128.

7. **3-Me 4-NO_2 Phenol**: ^{1}H NMR (300 MHz, $CDCl_3$): δ 10.64 (s, 1H, OH), 2.35 (s, 3H, Me), 6.85 (d, 1H, $J = 8$ Hz), 8.12 (d, 1H, $J = 8$ Hz), 6.76 (s, 1H); mp = 127–129°C; HRMS (EI) Calcd. M, 153.1351, Found: 153.0436.
8. **3-Cl 4-NO_2 Phenol**: ^{1}H NMR (300 MHz, $CDCl_3$): δ 10.28 (s, 1H, OH) 6.92 (d, 1H, $J = 8.5$ Hz), 7.35 (s, 1H), 8.16 (d, 1H, $J = 8.5$ Hz); mp = 117–120°C; HRMS (EI) Calcd. M, 173.5534, Found: 172.9889.
9. **4-NO_2 Benzene 1,3 diol**: ^{1}H NMR (300 MHz, $CDCl_3$): δ10.35 (s, 2H, OH), 7.82 (d, 1H, $J = 8$ Hz, $J = 7.5$ Hz), 7.12 (d, 1H, $J = 7.5$ Hz), 7.48 (s, 1H); mp = 124–127°C; HRMS (EI) Calcd. M, 155.1082 Found: 155.0218.
10. **2-Me 4-NO_2 Phenol**: ^{1}H NMR (300 MHz, $CDCl_3$): δ 10.55 (s, 1H, OH), 2.35 (s, 3H, Me), 6.85 (d, 1H, $J = 8.5$ Hz), 8.12 (d, 1H, $J = 8.5$ Hz), 8.25 (dd, 1H, $J = 8.5$ Hz, $J = 7.5$ Hz); mp = 95–98°C; HRMS (EI) Calcd. M, 153.1351 Found: 153.0415,
11. **4-NO_2 Benzene 1,2 diol**: ^{1}H NMR (300 MHz, $CDCl_3$): δ 10.24 (s, 2H, –OH), 6.95 (d, 1H, $J = 8.5$ Hz), 7.75 (d, 1H, $J = 8.5$ Hz), 7.48 (s, 1H); mp = 176–178°C;; HRMS (EI) Calcd. M, 155.1082, Found: 155.0222.

Computation of Activation Parameters

Rate constants increased substantially with an increase in the temperature. According to Eyring's theory of reaction rates [27], at any given temperature free energy of activation ($G^{\#}$) can be correlated to the rate constant (k),

$$k = (RT/Nh)\exp(-\Delta G^{\#}/RT) \qquad (5)$$

where R is the gas constant, h is the Plank's constant, N is the Avogadro's number, and T is the temperature in absolute scale. For convenience, a rearranged form of Eyring's equation can be given as

$$\Delta G^{\#} = RT\ln(RT/Nhk) \qquad (6)$$

Accordingly, the above equation is used to calculate the free energy of activation ($\Delta G^{\#}$) at various temperatures. Free energy of activation ($\Delta G^{\#}$) values thus obtained were further used in the Gibbs–Helmholtz plot of $\Delta G^{\#}$ versus T, using the following equation for the evaluation of enthalpy of activation ($\Delta H^{\#}$) and entropy of activation ($\Delta S^{\#}$), as shown in Tables I–V.

$$\Delta G^{\#} = \Delta H^{\#} - T\Delta S^{\#} \qquad (7)$$

All the TBN-mediated nitration of different phenols reactions have been studied in different solvent media at four to five temperatures in the 20°C range (303–323 K). The rate of nitration increased with an increase in temperature in different solvent media (MeCN, dichloroethane (DCE), CCl_4, dimethylformamide (DMF), and toluene).

Effect of Varying Solvent and Solvochromic Studies

Physical constants such as melting and boiling points, vapor pressure, heat of vaporization, refractive index, density, viscosity, surface tension, dipole moment, relative permittivity, polarizability, specific conductivity, etc. can be generally used to characterize the properties of a solvent. Literature reports revealed that change in the nature of solvent may influence the reaction rate alone with or without influencing the mechanism [28–32]. Solvents can affect rates through equilibrium-solvent or frictional-solvent effects [28].

1. Equilibrium-Solvent effects.

Equilibrium solvent effects are based on the transition state theory. When the reactant molecules proceed to the transition state, the solvent molecules orient themselves to stabilize the transition state. If the solvent stabilizes the transition state more effectively than the stabilization of reactants then the reaction proceeds faster. If the solvent stabilizes starting material more effectively than the transition state then the reaction proceeds slower. However, such differential solvation requires rapid reorientational relaxation of the solvent (from the transition state orientation back to the ground-state orientation).

2. Frictional-solvent effects.

The equilibrium hypothesis does not stand for very rapid chemical reactions in which the transition state theory breaks down. In such cases involving strongly dipolar, slowly relaxing solvents, solvation of the transition state does not play a very large role in affecting the reaction rate. Instead, dynamic contributions of the solvent (such as friction, density, internal pressure, or viscosity) play a large role in affecting the reaction rate.

To establish the nature of reactive species, the reactions and effect of solvent on the rate of nitration, kinetics of the reactions have been studied in

Table I Second-Order Rate Constants and Activation Parameters in MeCN Medium

Substrate	Temperature (K)	k	$\Delta G^{\neq}$ (kJ/mol)	Equation and R^2	$\Delta H^{\neq}$ (kJ/mol)	$-\Delta S^{\neq}$ (J/K/mol)
Phenol	303	0.215	78.12	$y = 200.44x + 17{,}501$	17.5	200
	313	0.253	80.36	$R^2 = 0.9955$		
	323	0.351	82.13			
p-Cresol	303	0.235	77.9	$y = 196.13x + 18{,}480$	18.48	196
	313	0.309	79.84	$R^2 = 0.9998$		
	323	0.393	81.83			
p-Cl phenol	303	0.165	78.79	$y = 179.55x + 24{,}357$	24.36	179
	313	0.23	80.61	$R^2 = 0.998$		
	323	0.329	82.31			
p-Br phenol	303	0.154	78.96	$y = 167.26x + 28{,}165$	28.17	167
	313	0.242	80.47	$R^2 = 0.9934$		
	323	0.344	82.19			
Quinol	303	0.308	77.21	$y = 193.5x + 18{,}586$	18.59	193
	313	0.408	79.12	$R^2 = 0.9989$		
	323	0.508	81.14			
p-OMe phenol	303	0.256	77.68	$y = 193.5x + 18{,}868$	18.87	194
	313	0.387	79.25	$R^2 = 0.9906$		
	323	0.448	81.49			
p-NO_2 phenol	303	0.062	81.25	$y = 91.78x + 53{,}285$	53.29	92.0
	313	0.142	81.86	$R^2 = 0.9653$		
	323	0.248	83.06			
m-Cl phenol	303	0.112	79.76	$\mathrm{i} = 138.1x + 37{,}810$	37.81	138
	313	0.205	80.91	$R^2 = 0.9902$		
	323	0.303	82.53			
m-Cresol	303	0.233	77.92	$y = 190.8x + 20{,}160$	20.16	190
	313	0.287	80.03	$R^2 = 0.9962$		
	323	0.407	81.73			
Resorcinol	303	0.066	81.1	$y = 134.25x + 4028$	40.28	134
	313	0.134	82.01	$R^2 = 0.9677$		
	323	0.19	83.78			

different solvents by changing the reaction medium with a change in dielectric constant (D). Customarily, we have tried to interpret the kinetic results based on semiquantitative relationships developed by Amis, Laidier–Eyring, Krikwood, Ingold, and others [29–33]. Laidler–Eyring's theory brought out a relationship between the rate of the reaction (or the rate constant) as a function of bulk dielectric constant (D).

$$\frac{d\ln(k')}{d(1/D)} = \frac{NZ^2e^2}{2RT}\left\{\frac{1}{r_A} - \frac{1}{r_\#}\right\} \tag{8}$$

where r_A and $r_\#$ represent the radii of the reactant ion and activated complex, respectively. Parameters N, Z, e, R, and T have their usual significance. The above equation shows that irrespective of the charge in the ion (negative or positive) the slope of the plot in k' versus ($1/D$) should be positive provided $r_A > r_\#$. For the possibility of a cationic species in the rate-limiting step r_A should be greater than $r_\#$. For ion–ion reactions, the Ingold rule [31] states that the reaction proceeds faster in a solvent of low dielectric constant. Reactions, which could not obey Laidler–Eyring theory and Ingold rule, the Amis equation [32] could be applied,

$$\log k' = \log k + \frac{NZed_o}{2.303 \quad RTr_o^2D} \tag{9}$$

where d_o is the dipolement of a dipolar molecule, k is the rate constant in a medium of infinite dielectric constant, r_o is the distance of closest approach for the ion and a molecule to react, and other parameters depict their usual significance.

At constant ionic strength (μ), Amis equation, predicts that the plot of log k versus ($1/D$) should be a straight line with a positive slope if z is positive and negative if z is negative. If Amis plots give a negative slope, it clearly rules out the participation of a cationic species. For the reactions between neutral

Table II Second-Order Rate Constants and Activation Parameters in DMF Medium

Substrate	Temperature (K)	k	$\Delta G^{\neq}$ (kJ/mol)	Equation and R^2	$\Delta H^{\neq}$ (kJ/mol)	$-\Delta S^{\neq}$ (J/K/mol)
Phenol	303	0.116	79.67	$y = 120.81x + 42{,}854$	42.85	120
	313	0.24	80.5	$R^2 = 0.9632$		
	323	0.36	82.06			
p-Cresol	303	0.143	79.15	$y = 136.81x + 37{,}414$	37.41	136
	313	0.296	79.95	$R^2 = 0.9515$		
	323	0.394	81.82			
p-Cl phenol	303	0.104	79.95	$y = 126.55x + 41{,}420$	41.42	126
	313	0.215	80.78	$R^2 = 0.9654$		
	323	0.307	82.49			
p-Br phenol	303	0.102	79.99	$y = 130.52x + 40{,}175$	40.18	0.13
	313	0.216	80.77	$R^2 = 0.9512$		
	323	0.302	82.54			
Quinol	303	0.196	78.35	$y = 139.55x + 35{,}800$	35.8	139
	313	0.374	79.34	$R^2 = 0.9635$		
	323	0.525	81.05			
p-OMe phenol	303	0.176	78.62	$y = 139.79x + 36{,}056$	36.06	139
	313	0.343	79.57	$R^2 = 0.9689$		
	323	0.46	81.41			
p-NO_2 phenol	303	0.058	81.42	$y = 103x + 49{,}997$	49.99	103
	313	0.131	82.07	$R^2 = 0.9538$		
	323	0.216	83.44			
m-Cl phenol	303	0.082	80.55	$y = 117.93x + 44{,}678$	44.68	117
	313	0.175	81.32	$R^2 = 0.9614$		
	323	0.263	82.91			
m-Cresol	303	0.124	79.51	$y = 110.74x + 45{,}812$	45.81	110
	313	0.27	80.19	$R^2 = 0.9534$		
	323	0.409	81.72			
Resorcinol	303	0.161	78.85	$y = 108.58x + 45{,}815$	45.82	108
	313	0.348	79.53	$R^2 = 0.9557$		
	323	0.531	81.02			

molecules (dipole–dipole type), forming an activated complex more polar than the reactants, Kirkwood's theory [27,33] predicts the following relationship,

$$\ln k' = \ln k_o - \frac{N}{RT}\left(\frac{D-1}{2D+1}\right)\left(\frac{d_A^2}{r_A^3}+\frac{d_B^2}{r_B^3}+\frac{d_\#^2}{r_\#^3}\right) \tag{10}$$

where k' is the specific rate constant, d_A, d_B, and $d_\#$ are the dipole moments of reactants A, B, and the activated complex, respectively. The above equation predicts that the rate should decrease with a decrease in D of the medium. When the rate data are tested with the plots of log k'' versus ($1/D$) or [($D - 1$)/($2D + 1$)] were not linear and gave poor correlation coefficients:

$$\text{Amis plots : } \log k' \text{ versus } (1/D) :$$

$$y = -0.158\text{itx} - 0.058;\ R^2 = 0.397\,(\text{phenol}) \tag{11a}$$

$$y = -0.870x - 0.001;\ R^2 = 0.281\,(p\text{−cresol}) \tag{11b}$$

$$\text{Kirkwood Plots : } \log k' \text{ versus } (D - 1/2D + 1) :$$

$$y = 0.112x + 0.540;\ R^2 = 0.396\,(\text{phenol}) \tag{12a}$$

$$y = 0.085x + 0.500;\ R^2 = 0.285\,(p - \text{Cresol}) \tag{12b}$$

These observations probably indicate that apart from dielectric constant, other solvent properties might be important in controlling the reaction rates. Robinson and Stokes earlier stated that "the bulk dielectric constant is entirely different from internal dielectric constant especially in the solvent of low dielectric media" [28]. Brown and Hudson have found that the rate of hydrolysis of acid chlorides in DMF is almost equal to 95% dioxane in spite of the difference in their dielectric constants. A perusal of literature depicts

Table III Second-Order Rate Constants and Activation Parameters in CCl_4 Medium

Substrate	Temperature (K)	k	$\Delta G^{\neq}$ (kJ/mol)	Equation and R^2	$\Delta H^{\neq}$ (kJ/mol)	$-\Delta S^{\neq}$ (J/K/mol)
Phenol	303	0.238	77.86	$y = 198.3x + 17{,}682$	17.68	198
	313	0.322	79.73	$R^2 = 0.9976$		
	323	0.397	81.80			
p-Cresol	303	0.395	76.59	$y = 207.1x + 13{,}795$	13.8	207
	313	0.507	78.55	$R^2 = 0.9985$		
	323	0.587	80.75			
p-Cl phenol	303	0.064	81.17	$y = 121.3x + 44{,}220$	44.22	121
	313	0.132	82.05	$R^2 = 0.9631$		
	323	0.2	83.64			
p-Br phenol	303	0.066	81.1	$y = 122.9x + 43{,}644$	43.64	122
	313	0.136	81.97	$R^2 = 0.9604$		
	323	0.205	83.58			
Quinol	303	0.947	74.38	$y = 178.2x + 20{,}264$	20.26	0.178
	313	1.312	76.08	$R^2 = 0.9943$		
	323	1.684	77.92			
p-OMe phenol	303	1.086	74.04	$y = 206.83x + 11{,}438$	11.44	0.206
	313	1.245	76.21			
	323	1.503	78.23	$R^2 = 0.9989$		
m-Cl phenol	303	0.033	82.84	$y = 108.64x + 49{,}847$	49.88	0.108
	313	0.07	83.70	$R^2 = 0.9859$		
	323	0.12	85.01			
m-Cresol	303	0.16	78.86	$y = 149.23x + 33{,}659$	33.66	0.149
	313	0.25	80.39	$R^2 = 0.9998$		
	323	0.39	81.85			
Resorcinol	303	1.341	73.51	$y = 207.55x + 10{,}587$	10.59	0.207
	313	1.651	75.48	$R^2 = 0.9991$		
	323	1.856	77.66			

several such anomalies. Many reactions are over a million times faster in dipolar aprotic solvents such as *N*,*N*′-dimethyl formamide (DMF) than in protic solvents of much the same dielectric constant.

Shorter's book on correlation analysis provided striking examples on the role of dielectric constant effects on chemical reactivity [34], which enlighten the fact that apart from the dielectric constant of the medium, solvent–solute interactions are also equally responsible or sometimes more important in affecting the reaction rates and mechanisms; and the role of solvent in a chemical reaction is conditioned not only by its chemical constitution but also the type of reaction taking place in it. The rates and mechanisms may also change due to solvation, and other solvent properties such as nucleophilicity, electrophilicity, solvolysis, hydrogen bonding tendency, basicity etc. The influence of solvent depends on the nature of reactive species. Electrostatic forces of interaction become very important in the reactions involving ions and Van der Waals forces become predominant in reactions involving neutral molecules. Besides solvation of ionic species, ion–ion, ion–dipole, dipole–dipole interaction, salvation of molecular species, and solvent–solute interactions also become important in affecting the rates and mechanisms of reactions. Unfortunately, there is no direct logical connection between the macroscopic solvent parameters that are used in solvent effects and microscopic details of reaction processes. The effect of solvent on the reactivities may be understood from the stand point of a specific solvation effect and a nonspecific solvation effect. To establish such a connection, two main methods for the examination of the solvent effects on the reaction rates have been developed. Several pioneers in the field of physical organic chemistry research set out general equations for the correlations of solvent effects through multiple regression analysis. Either the rate constants (log *k*) or the free energies of activation ($\Delta G^{\#}$) may be correlated with a characteristic physical parameter of the solvent such as dielectric constant, solubility parameter, viscosity, etc. [34–37]. Notably, Mather and Shorter [38] on the reaction of diazodiphenylmethane and benzoic acid and more generally by Koppel and Palm [39], Kamlet and Taft and their

Table IV Second-Order Rate Constants and Activation Parameters in Toluene Medium

Substrate	Temperature (K)	k	$\Delta G^{\neq}$ (kJ/mol)	Equation and R^2	$\Delta H^{\neq}$ (kJ/mol)	$-\Delta S^{\neq}$ (J/K/mol)
Phenol	303	0.213	78.14	$y = 163.82x + 28{,}353$	28.35	163
	313	0.345	79.55	$R^2 = 0.9913$		
	323	0.47	81.35			
p-Cresol	303	0.247	77.77	$y = 164.88x + 27{,}560$	27.56	164
	313	0.416	79.07	$R^2 = 0.9769$		
	323	0.543	80.96			
p-Cl phenol	303	0.139	79.22	$y = 152.57x + 32{,}853$	32.85	152
	313	0.242	80.47	$R^2 = 0.991$		
	323	0.339	82.23			
p-Br phenol	303	0.134	79.31	$y = 146.25x + 34{,}780$	34.78	146
	313	0.25	80.39	$R^2 = 0.9715$		
	323	0.338	82.23			
Quinol	303	0.355	76.86	$y = 191.85x + 18{,}649$	18.65	191
	313	0.498	78.6	$R^2 = 0.9975$		
	323	0.601	80.69			
p-OMe phenol	303	0.281	77.45	$y = 169x + 25{,}975$	25.98	169
	313	0.498	78.6	$R^2 = 0.9686$		
	323	0.575	80.81			
p-NO_2 phenol	303	0.068	81.02	$y = 167.86x + 30{,}021$	30.02	167
	313	0.11	82.53	$R^2 = 0.9917$		
	323	0.153	84.36			
m-Cl phenol	303	0.112	79.76	$y = 139.98x + 37{,}272$	37.27	140
	313	0.203	80.93	$R^2 = 0.991$		
	323	0.299	82.56			
m-Cresol	303	0.189	78.44	$y = 162.84x + 29{,}093$	29.09	162
	313	0.286	80.04	$R^2 = 0.9999$		
	323	0.412	81.70			
Resorcinol	303	0.056	81.51	$y = 208.04x + 18{,}587$	18.59	208
	313	0.064	83.94	$R^2 = 0.9908$		
	323	0.094	85.67			

co-workers [40–45] have extended this type of analysis to multiple linear correlations with a number of solvent parameters. In the second method, the solvent effect on log k or $\Delta G^{\#}$ is the contributions of the reactants (initial state) and the transition state, followed, where possible, by a comparison of solvent effects on the transition state with solvent effects on solutes that might function as suitable models for the transition state. Koppel and Palm [39] used the four-parameter equation:

$$\log k = \log k_0 + g f(\mathrm{D}) + p f(n) + eE + bB \qquad (13)$$

In this equation, $f(D)$ is a dielectric constant function [usually $f(D) = (D - 1)/(2D + 1)$], $f(n)$ is a refractive index function, $(n^2 - 1)/(n^2 + 2)$, and E and B are measures of the electrophilic and nucleophilic solvation ability of the solvent, respectively. Koppel and Palm [39] and later Mather and Shorter [38] quite successfully applied Eq. (13) to a variety of reaction types.

Koppel and Palm's Linear Solvation Energy Relationship in TBN-Mediated Nitration. Based on the foregoing discussion on solvent energy relationships, we have used a basic form of Koppel and Palm's multivariate linear solvent energy relationship (MLSER) to explain the multiple interacting effects of the solvent on the reactivity of substrates in the nitration of phenols:

$$\log k = p_1 \pi * + p_2 \alpha + p_3 \beta + p_4 \delta + \text{constant} \qquad (14)$$

where $\pi* =$ solvent dipolarity/polarizability; $\alpha =$ hydrogen bond donor (HBD); $\delta =$ hydrogen bond acceptor (HBA) basicity parameter; $\delta =$ Hildebrand solubility parameter,; and p_1, p_2, p_3, and p_4 are corresponding coefficients. Multiple linear regression analysis (MLRA) of the kinetic data pertains to the nitration of phenols in various solvents furnished the parameters p_1, p_2, p_3, and p_4. These values are compiled in Table VI as a typical example. (Similar observations

Table V Second-Order Rate Constants and Activation Parameters in DCE Medium

Substrate	Temperature (K)	k	$\Delta G^{\neq}$ (kJ/mol)	Equation and R^2	$\Delta H^{\neq}$ (kJ/mol)	$-\Delta S^{\neq}$ (J/K/mol)
Phenol	303	0.163	78.82	$y = 163.86x + 29{,}018$ $R^2 = 0.9793$	29.02	163
	313	0.288	80.02			
	323	0.351	82.13			
p-Cresol	303	0.135	79.29	$y = 152.1x + 33{,}042$ $R^2 = 0.9869$	33.04	152
	313	0.238	80.52			
	323	0.325	82.34			
p-Cl phenol	303	0.183	78.53	$y = 151.87x + 32{,}246$ $R^2 = 0.9702$	32.25	151
	313	0.338	79.61			
	323	0.454	81.44			
p-Br phenol	303	0.198	78.33	$y = 165x + 28{,}206$ $R^2 = 0.9921$	28.21	165
	313	0.326	79.7			
	323	0.427	81.61			
Quinol	303	0.109	79.83	$y = 149.11x + 34{,}390$ $R^2 = 0.97$	34.39	149
	313	0.205	80.91			
	323	0.283	82.71			
p-OMe phenol	303	0.113	79.74	$y = 118.88x + 43{,}668$ $R^2 = 0.9851$	43.67	118
	313	0.218	80.75			
	323	0.342	82.20			
p-NO_2 phenol	303	0.284	77.42	$y = 153.94x + 30584$ $R^2 = 0.9799$	30.58	154
	313	0.508	78.55			
	323	0.653	80.46			
m-Cl phenol	303	0.224	78.02	$y = 172.69x + 25513$ $R^2 = 0.9695$	25.51	172
	313	0.393	79.21			
	323	0.449	81.47			
m-Cresol	303	0.142	79.16	$y = 151.05x + 33{,}198$ $R^2 = 0.9502$	33.2	151
	313	0.282	80.08			
	323	0.344	82.19			
Resorcinol	303	0.1	80.05	$y = 106.88x + 47{,}701$ $R^2 = 0.9963$	47.70	106
	313	0.181	81.23			
	323	0.344	82.19			

are made at other temperatures that are presented in Tables AI–AVI). For instance, the data for nitration of phenol at 303 K depicted in the following equations:

$$\log k = 0.229\pi* + 0.201\,\alpha - 0.263\,\beta - 0.936; \quad R^2 = 0.684 \quad (15)$$

(when Hildebrand solubility parameter, δ, is eliminated)

$$\log k = 0.269\pi* + 0.063\,\alpha + 0.021\delta - 1.128; \quad R^2 = 0.586 \quad (16)$$

(when HBA/basicity parameter, β, is eliminated)

$$\log k = 0.300\pi* + 0.263\beta - 0.021\delta + \text{constant}; \quad R^2 = 0.679 \quad (17)$$

(when HBA/acidity parameter, α, is eliminated)

$$\log k = 0.257\,\pi* + 0.024\,\delta + \text{constant}; \quad R^2 = 0.585 \quad (18)$$

(when parameters, α and β are eliminated)

A perusal of the computed results in Eqs. (15)–(18) clearly revealed poor correlation coefficients (far less R^2 values form linearity), indicating that none of the Koppel and Palm's basic solvent parameters (π*, α, β, and δ) alone are responsible for the solvation of the transition state during nitration of phenols. When the entire basic parameters are used in the regression analysis, excellent linearity is obtained with a correlation coefficient of unity ($R^2 = 1.00$) as shown in Eq. (15). This observation probably strengthens our view that cumulative contributions of basic solvent parameters

Table VI Applicability of MLSER for Para-Substituted Phenols 303 K

Substrate	p_1	p_2	p_3	p_4	Constant	R^2	Remarks
Phenol	0.829	2.124	1.061	–0.263	1.106	1	Considering all parameters
	0.229	0.201	0.189	–	–0.936	0.684	Parameter δ excluded
	0.269	0.063	–	0.021	–1.128	0.586	Parameter β excluded
	0.300	–	0.263	–0.021	–0.778	0.679	Parameter α excluded
	0.257	–	–	0.024	–1.150	0.585	Parameters α and β excluded
p-Cresol	0.524	1.954	1.564	–0.273	1.369	1	Considering all parameters
	–0.099	–0.042	–	–	–0.751	0.852	Parameters δ and β excluded
	0.038	–	–	–0.50	–0.364	0.882	Parameter α and β excluded
	0.097	–	0.830	0.090	–1.539	0.473	Parameter α excluded
p-Cl phenol	0.736	1.931	–0.286	–0.130	–0.062	1	Considering all parameters
	0.438	0.977	–0.719	–	–1.074	0.963	Parameter δ excluded
	0.887	2.488	–	–0.207	0.541	0.986	Parameter β excluded
	0.255	–	–1.012	0.090	–1.774	0.874	Parameter α excluded
	0.420	–	–	–0.082	–0.341	0.211	Parameters α and β excluded
p-Br phenol	0.779	1.749	–0.498	–0.112	–0.238	1	Considering all parameters
	0.522	0.927	–0.870	–	–1.110	0.980	Parameter δ excluded
	1.0422	2.716	–	–0.245	0.810	0.968	Parameter β excluded
	0.343	–	–1.155	0.087	–1.788	0.923	Parameter α excluded
	0.532	–	–	–0.109	–0.153	0.280	Parameters α and β excluded
Quinol	0.264	2.279	2.561	–0.356	2.296	1	Considering all parameters
	–0.548	–0.324	1.381	–	–0.468	0.923	Parameter δ excluded
	–1.088	–2.669	–	0.329	–3.097	0.679	Parameter β excluded
	–0.303	–	1.705	–0.096	0.275	0.951	Parameter α excluded
	–0.581	–	–	0.193	–2.140	0.424	Parameters α and β excluded
p-OMe phenol	0.084	0.790	2.153	–0.214	1.070	1	Considering all parameters
	–0.404	–0.773	1.444	–	–0.590	0.975	Parameter δ excluded
	–1.052	–3.394	–	0.362	–1.3463	0.799	Parameter β excluded
	–0.112	–	1.856	–0.124	0.370	0.995	Parameter α excluded
	–0.415	–	–	0.192	–2.259	0.442	Parameters α and β excluded

might be responsible for solvation.

$$\log k = 0.829\,\pi{*} + 2.124\,\alpha + 1.061\,\beta - 0.263\,\delta + 1.106;\ R^2 = 1.00 \qquad (19)$$

The coefficients corresponding to different variables (π*, α, β, and δ) further reveal that apart from solvent dipolarity/polarizability (π*), HBD and HBA properties (α, β), and Hildebrand solubility parameter (δ) are contributing substantially for the solvation of transition state. The positive magnitudes of coefficients p_2 and p_3 ($+$ 2.124α, $+$ 1.061β) may probably indicate the favorable attack of the nitronium ion at the electron-rich benzene ring to afford a nitro derivative.

It is of interest to note that similar results are obtained for other phenols, which can be readily seen from Table VI (for other tables, refer to Tables AI–AVI in the Appendix).

Kamlet and Taft's Multivariate Linear Solvent Energy Relationship. Kamlet and Taft's group and others [41–43] modified original form of Koppel and Palm's "MLSER" as shown in the following equation:

$$\log k = A_0 + s\pi{*} + a\alpha + b\beta \qquad (20)$$

where π*, β, and α represent their usual scale of the solvent. The coefficients *s*, *a*, and *b* measure the relative susceptibilities of the solvent-dependent solute property (log *k* or as $\Delta G^{\#}$) to the corresponding solvent parameters. However, to have further insight into the solvation, we have designed another "MLSER" using equilibrium and frictional solvent effects, as shown in Eq. (2).

$$\log k = m_1\varphi_1 + m_2\varphi_2 + m_3\varphi_3 + m_4\varphi_4 + \text{constant} \qquad (21)$$

Table VII Kamlet and Taft's MLSER at 303 K

Substrate	m_1	m_2	m_3	m_4	Constant	R^2	Remarks
Phenol	0.711	–0.075	–0.166	–0.433	–0.432	1	Using all parameters
	8.883	0.191	7.198	–	–6.978	0.951	Parameter ϕ_4 excluded
	0.892	–0.069	–	–0.424	–0.577	1	Parameter ϕ_3 excluded
	2.941	–	1.891	–0.318	–2.230	0.996	Parameter ϕ_2 excluded
p-Cl phenol	35.6	1.464	35.108	2.099	30.924	1	Using all parameters
	–4.024	0.076	–0.599	–	0.815	0.455	Parameter ϕ_4 excluded
	–2.479	0.243	–	0.209	–0.381	0.517	Parameter ϕ_3 excluded
	8.180	–	–5.289	–0.157	4.384	0.334	Parameter ϕ_2 excluded
m-Cresol	–2.216	0.022	–1.809	–0.280	0.976	1	Using all parameters
	3.071	0.194	2.956	–	–3.259	0.971	Parameter ϕ_4 excluded
	–0.255	0.085	–	–0.183	–0.598	0.996	Parameter ϕ_3 excluded
	–2.873	–	–2.415	–0.314	1.505	1	Parameter ϕ_2 excluded
Catechol	–72.372	–2.734	–61.995	–3.825	57.112	1	Using all parameters
	–0.169	–0.386	3.071	–	–0.722	0.656	Parameter ϕ_4 excluded
	–5.131	–0.578	–	–0.487	3.179	0.714	Parameter ϕ_3 excluded
	9.388	–	13.447	0.388	–8.826	0.559	Parameter ϕ_2 excluded
Quinol	–64.450	–2.496	–62.038	–4.228	53.700	1	Using all parameters
	16.504	0.136	10.914	–	–11.144	0.364	Parameter ϕ_4 excluded
	2.838	–0.339	–	–0.948	–0.271	0.579	Parameter ϕ_3 excluded
	10.202	–	6.845	–0.441	–6.506	0.459	Parameter ϕ_2 excluded
o-Cresol	47.712	1.372	41.480	2.358	–7.996	1	Using all parameters
	3.190	–0.075	1.360	–	–2.335	0.178	Parameter ϕ_4 excluded
	2.722	–0.071	–	0.125	–1.910	0.196	Parameter ϕ_3 excluded
	6.681	–	3.620	0.244	–4.906	0.302	Parameter ϕ_2 excluded
Resorcinol	–50.010	–2.943	–61.909	–3.684	46.801	1	Using all parameters
	19.538	–0.681	0.764	–	–8.906	0.819	Parameter ϕ_4 excluded
	17.138	–0.789	–	–0.351	–7.058	0.838	Parameter ϕ_3 excluded
	37.986	–	19.287	0.850	–24.167	0.710	Parameter ϕ_2 excluded
p-Cresol	–23.531	–1.049	–25.124	–1.953	21.325	1	Using all parameters
	11.333	0.149	8.096	–	–8.202	0.568	Parameter ϕ_4 excluded
	1.719	–0.175	–	–0.600	–0.532	0.774	Parameter ϕ_3 excluded
	5.843	–	3.826	–0.336	–3.977	0.687	Parameter ϕ_2 excluded

where ϕ_1 is the dielectric constant function, $(D - 1)/(2D + 1)$; ϕ_2 is the viscosity function, 1/viscosity; ϕ_3 is the refractive index function, $(\eta^2 - 1)/(\eta^2 + 2)$; and ϕ_4 is the density, whereas m_1, m_2, m_3, and m_4 are corresponding coefficients. Furthermore, ϕ_1 and ϕ_3 indicate equilibrium solvent parameters whereas ϕ_2 (reciprocal of viscosity) and ϕ_4 (density) indicate frictional solvent properties. Statistical analysis using "multiple linear regression technique" afforded parameters under different conditions. The coefficients m_1, m_2, m_3, and m_4 corresponding to ϕ_1, ϕ_2, ϕ_3, and ϕ_4 and correlation coefficients (R^2 values) are presented in Table VII as a typical example (for other data, refer to AVII–AX in the Appendix). A perusal of the computed results (using Eq. (17)), which are given in Table VII, clearly show that when all solvent parameters (ϕ_1, ϕ_2, ϕ_3, and ϕ_4) are used in the regression analysis excellent linearity is obtained with a correlation coefficient of unity ($R^2 = 1.00$). However, except for phenol and *m*-cresol, in all other cases regression analysis afforded poor correlation coefficients ($R^2 <$ 0.900 or even lesser than this value) when any one of the solvent parameters is excluded from the analysis. This observation probably strengthens our view once again cumulative contributions of basic solvent parameters might be responsible for solvation. In addition, to this the observed results may also indicate the importance of equilibrium as well as frictional solvent effects and solvent–solute interactions for solvation of transition state during nitration of phenols.

Quantitative Structure Reactivity Study.

Hammett's Plots. A closer look into the kinetic data pertaining to the TBN nitration of phenols revealed that the reaction is sensitive to the structural variation

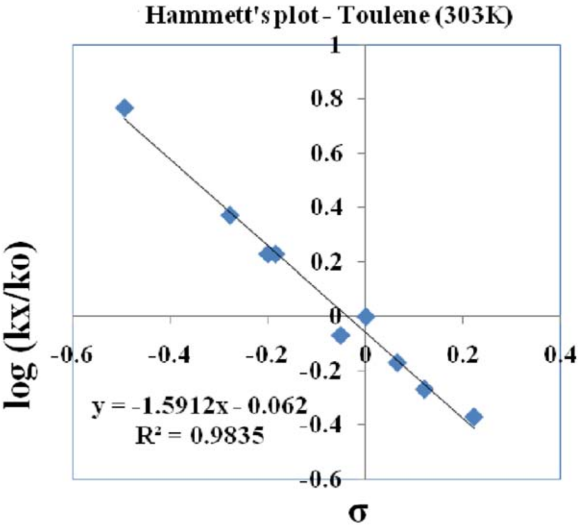

Figure 5 Hammett's plots at 303 K in toluene.

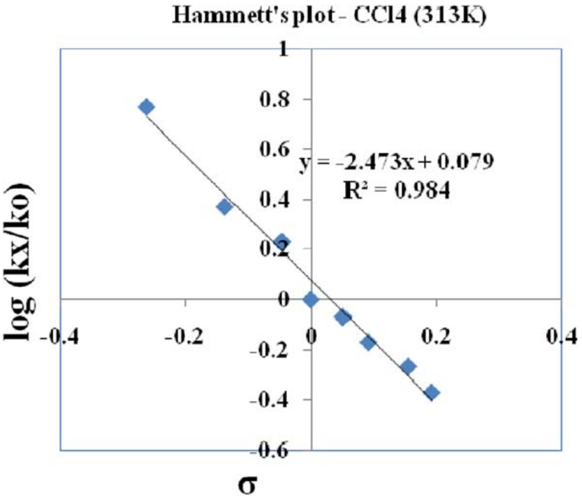

Figure 6 Hammett's plot at 313 K in CCl_4.

of phenol. Reaction rates accelerated with the introduction of electron-donating groups and retarded with electron-withdrawing groups. Accordingly, the reactivity of structurally different phenols was found to follow the sequence: *p*-OH > *p*-MeO > p-Me > H > *m*-Me > *p*-Cl > *p*– Br > *m*-Cl > *p*–NO_2 > *m*–OH. Hammett's theory of linear free energy relationships furnishes an efficient tool to analyze the kinetic data quantitatively that is useful to understand the mechanism of a reaction [46]. According to Hammett's relationship, the rate or equilibrium constant for a reaction of a compound varies as a function of sigma (σ), the substituent constant.

$$\log(k/k0) = \sigma\ \rho \tag{22}$$

The value of sigma (σ) of a substituted compound differs from that of the parent compound. This depends on the nature of substituent. In the present study, Hammett's plots of log(k/k_0) versus σ (Figs. 5–7) exhibited a very good linear relationship as evidenced from the correlation coefficient values (R^2), which were greater than 0.960. The negative value of ρ indicates that electron-donating substituent accelerates the reaction rate. A negative ρ value also indicates the electron flow away from aromatic ring takes place in the rate-determining step and thus produces electron deficiency (often a positive charge) in the activated complex.

Rho (ρ) Values for Various Electrophilic Substitutions. The rate-determining step for most electrophilic substitutions is the attack step in which the electrophile reacts with the aromatic to form the arenium ion. The degree to which the Transition State (TS) for this reaction resembles the arenium ion is a major determinant of the size of the rho value for a particular type of electrophilic substitution. For bromination, the rho value is quite large (–12.1), indicating a TS which strongly resembles the arenium ion. This is consistent with the accepted mechanism, in which

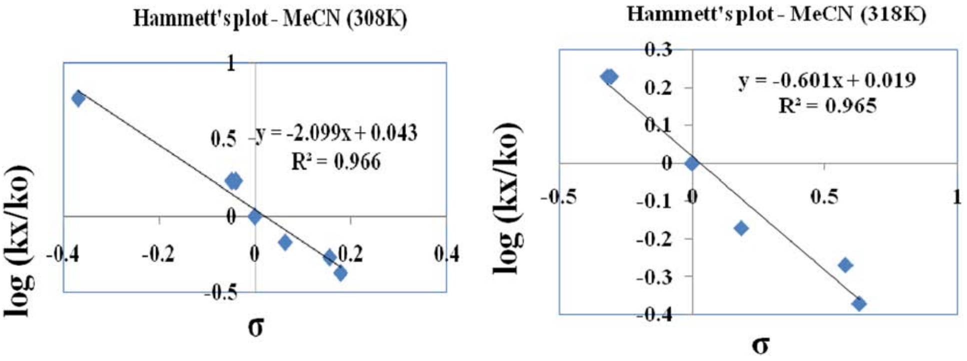

Figure 7 Hammett's plots at 308 K and 318 K in MeCN.

Table VIII Effect of Temperature/Solvent on Hammett's Reaction Constant (ρ)

Solvent	Temperature (K)	Hammett's ρ	Equation	β (K)
MeCN	303	–1.584	$y = 10202x - 35.19$	290
	308	–2.099	$R^2 = 0.978$	
	313	–2.49		
	318	–2.97		
	323	–3.76		
DMF	303	–0.461	$y = 798.4x - 3.104$	257
	308	–0.520	$R^2 = 0.984$	
	313	–0.556		
	318	–0.601		
	323	–0.624		
CCl_4	303	–2.165	$y = 372.3x - 14.41$	258
	308	–2.280	$R^2 = 0.980$	
	313	–2.473		
	318	–2.745		
	323	–2.885		
Toluene	303	–1.591	$y = 142.1x - 6.260$	227
	308	–1.644	$R^2 = 0.945$	
	313	–1.673		
	318	–1.793		
	323	–1.881		

neutral bromine is the (relatively mild) electrophile, so that the attack step is strongly endothermic. In Friedel-Crafts acylation, where the active electrophile is the acylium cation, the rho value decreases to –9.1. The rho value for nitration in acetonitrile is –6.2. The reaction constant (Hammett's ρ) is a measure of the sensitivity of the reaction toward the electronic effects of the substituent. Data presented in Table VIII revealed that the rho (ρ) values obtained from the present experiments are fairly large negative values ($\rho < 0$), indicating attack of an electrophile on the aromatic ring. Increase in temperature decreases the reaction constant (ρ) values. This trend is quantitatively represented according to the following relationship, as mentioned by Exner [47]:

$$\rho = A[1 - \beta/T] \qquad (23)$$

where A is a constant and β is the isokinetic temperature. When $\beta = T$, $\rho = 0$, thus isokinetic temperature is the temperature at which the effect of substituent on the rate of reaction vanishes and all the substituted compounds in a given series have the same reactivity.

Obtained "isokinetic temperature (β)" values are in the range of 225–290, as can be seen from Table VIII. These values are far below the experimental temperature range (303–323 K), indicating that the entropy factors are probably more important in controlling the reaction. Even though, the concept of isokinetic temperature (β) has been criticized by Peterson, Cornish-Bowden, and others [48], multivariate linear solvatochromic effects coupled with isokinetic temperature values certainly support our contention that entropy factors are important in controlling nitration of phenols by TBN in the present study.

Ortho Effect. Hammett introduced substituent constants, which are primarily derived from the ionization of substituted benzoic acids to quantify substituent effects. These constants successfully explained the reactivities of a variety of aromatic molecules, when the substituent is present at the meta or para position with respect to the reaction center. On the other hand, the Hammett's substituent constants for ortho substitution have been rarely used to explain the chemical reactivity as they failed in many cases due to interplay with proximity effects at the reaction center. Taft developed an equation in 1952 as a modification to the Hammett equation [49,50]. While the Hammett equation accounts for how field, inductive, and resonance effects influence reaction rates, the Taft equation describes the steric effects of a substituent. Taft's equation is a linear free energy relationship used in physical organic chemistry in the development of quantitative structure activity relationships for ortho-substituted aromatic compounds and aliphatic organic compounds and there by elucidating the reaction mechanisms.

The Taft equation is written as

$$\log(k/k_{CH_3}) = \rho{*}\sigma{*} \qquad (24)$$

Basically, it is customary to cast the rate data into Taft's polar substituent equation, considering only polar effects. If polar effects do not control the reaction then a linear correlation between log k and σ^* (polar substituent constant) could not be established. In such a case, rate data are cast into Taft's steric substituent equation:

$$\log(k/k_{\mathrm{CH3}}) = \delta\, E_s \tag{25}$$

If steric effects control the reaction then a linear correlation between log k and E_s (steric substituent constant) could be established. If both steric as well polar effects are important then the data are tested using the following equation:

$$\log(k/k_{\mathrm{CH_3}}) = \rho{*}\sigma{*} + \delta\, E_s \tag{26}$$

where log(k/k_{CH3}) is the ratio of the rate of the substituted reaction compared to the reference reaction, σ^* is the polar substituent constant that describes the field and inductive effects of the substituent, E_s is the steric substituent constant, ρ^* is the sensitivity factor for the reaction to polar effects, and δ is the sensitivity factor for the reaction to *steric* effects. In the present study, Taft's plots of log(k/k_{CH3}) versus σ^* or, log(k/k_{CH3}) versus E_s or combined did not give good correlations.

Charton Analysis. In view of the failure of Taft's equation, efforts were made to interpret the results using Charton analysis [50], by using the following set of equations:

$$\log k = a_1\,\sigma_{\mathrm{I}} + a_2\sigma_R + a_3\upsilon + \text{constant} \tag{27}$$

Where σ_{I} is the inductive constant of substituent**;** σ_R is the mesomeric/resonance constant; υ is the steric substituent constant; and $a_{1,}$ $a_{2,}$ and $a_{3,}$ are corresponding coefficients. Therefore, Eq. (27) has been modified by introducing a molar refractivity parameter (MR) and hydrophobicity parameter (π), respectively, as shown in Eqs. from (28) to (30), respectively.

$$\log k = a_1\sigma_{\mathrm{I}} + a_2\sigma_R + a_3\upsilon + a_4\,\mathrm{MR} + \text{constant} \tag{28}$$

$$\log k = a_1\sigma_{\mathrm{I}} + a_2\sigma_R + a_3\upsilon + a_5\pi + \text{constant} \tag{29}$$

$$\log k = a_1\sigma_{\mathrm{I}} + a_2\sigma_R + a_3\upsilon + a_4\mathrm{MR} + a_5\pi + \text{constant} \tag{30}$$

For instance, MLRA of the kinetic data pertains to the nitration of phenols in acetonitrile at 303 K depicted in the following set of equations:

$$\log k = 2.8396\,\sigma{*} + 4.1084;\ R^2 = 0.1585 \tag{31}$$

(basic Taft's polar equation when only polar substituent constant, σ^*, is taken into account.)

$$\log k = 2.01216\, E_s + 2.5312;\ R^2 = 0.284 \tag{32}$$

(basic Taft's steric equation when only steric substituent constant, $E_{s,}$ is taken into account)

$$\log k = -0.005\,\sigma{*} + 0.148\, Es - 0.896;\ R^2 = 0.285 \tag{33}$$

(when both Taft's polar and steric effects are considered)

$$\log k = -0.037\,\sigma_{\mathrm{I}} + 0.885\,\sigma_R + 0.333\upsilon - 0.729;\quad R^2 = 0.780 \tag{34}$$

(when Charton's polar, resonance and steric parameters are considered)

$$\log k = -0.126\,\sigma_{\mathrm{I}} + 0.870\,\sigma_R + 0.124\upsilon + 0.224\,\mathrm{MR} - 0.760;\ R^2 = 0.812 \tag{35}$$

(when Charton's polar, resonance, steric, and molar refractivity parameters are considered)

$$\log k = -0.249\,\sigma_{\mathrm{I}} + 0.579\,\sigma_R - 0.334\upsilon + 0.280\,\pi - 0.648;\ R^2 = 0.967 \tag{36}$$

(when Charton's polar, resonance, steric, and hydrophobicity parameters are considered)

A perusal of the computed results in Eqs. (31)–(36) clearly revealed poor correlation coefficients (far less R^2 values form linearity), indicating that that rate constant cannot be correlated to either Taft's (polar or steric parameters) or Charton's polar, resonance, steric, and hydrophobicity parameters to account for the nitration of ortho-substituted phenols. However, the correlation gradually increased from Taft's analysis to Charton analysis. It is reflected more so, from Eqs. (34) to (37) when basic parameters are considered gradually. Finally the regression analysis indicated very good used in linearity is obtained with correlation coefficient close to unity ($R^2 = 0.982$) as shown in Eq. (37). This observation probably strengthens our view that Charton's polar, resonance, steric, hydrophobicity,

Table IX Charton Analysis for Acetonitrile

Temperature (K)	Parameters	Equation	R^2
303	σ^*	$2.8396\sigma^* + 4.1084$	0.1585
	E_s	$2.01216E_s + 2.5312$	0.2839
	σ^*, E_s	$-0.005\sigma^* + 0.148\ E_s - 0.896$	0.285
	$\sigma_{\mathrm{I}}, \sigma_R, \upsilon$	$-0.037\sigma_{\mathrm{I}} + 0.885\sigma_R + 0.333\upsilon - 0.729$	0.780
	$\sigma_{\mathrm{I}}, \sigma_R, \upsilon$, MR	$-0.126\sigma_{\mathrm{I}} + 0.870\sigma_{\mathrm{R}} + 0.124\upsilon + 0.224\ \mathrm{MR} - 0.760$	0.812
	$\sigma_{\mathrm{I}}, \sigma_R, \upsilon, \pi$	$0.249\sigma_{\mathrm{I}} + 0.579\sigma_R - 0.334\upsilon + 0.280\pi - 0.648$	0.967
	$\sigma_{\mathrm{I}}, \sigma_R, \upsilon$, MR, π	$0.176\sigma_{\mathrm{I}} + 0.580\sigma_{\mathrm{R}} - 0.456\upsilon + 0.017\mathrm{MR} + 0.270\pi - 0.673$	0.982
313	σ^*	$5.0581\sigma^* + 5.2376$	0.2377
	E_s	$3.248E_s + 3.106$	0.3464
	σ^*, E_s	$0.007\sigma^* + 0.096E_s - 0.759$	0.349
	$\sigma_{\mathrm{I}}, \sigma_R, \upsilon$	$0.043\sigma_{\mathrm{I}} + 0.585\sigma_R + 0.215\upsilon - 0.647$	0.792
	$\sigma_{\mathrm{I}}, \sigma_R, \upsilon$, MR	$0.044\sigma_{\mathrm{I}} + 0.585\sigma_R + 0.217\upsilon + 0.00\ \mathrm{MR} - 0.647$	0.792
	$\sigma_{\mathrm{I}}, \sigma_R, \upsilon, \pi$	$0.241\sigma_{\mathrm{I}} + 0.374\sigma_R - 0.246\upsilon + 0.194\pi - 0.592$	0.981
	$\sigma_{\mathrm{I}}, \sigma_R, \upsilon$, MR, π	$0.265\sigma_{\mathrm{I}} + 0.373\sigma_R - 0.206\upsilon - 0.005\ \mathrm{MR} + 0.197\pi - 0.584$	0.984
323	σ^*	$5.9451\sigma^* + 5.1368$	0.2673
	E_s	$4.5446E_s + 3.4302$	0.5521
	σ^*, E_s	$-0.013\sigma^* + 0.141E_s - 0.650$	0.561
	$\sigma_{\mathrm{I}}, \sigma_R, \upsilon$	$0.096\sigma_{\mathrm{I}} + 0.543\sigma_R + 0.052\upsilon - 0.492$	0.872
	$\sigma_{\mathrm{I}}, \sigma_R, \upsilon$, MR	$0.094\sigma_{\mathrm{I}} + 0.543\sigma_R + 0.048\upsilon + 0.00\ \mathrm{MR} - 0.492$	0.872
	$\sigma_{\mathrm{I}}, \sigma_R, \upsilon, \pi$	$0.241\sigma_{\mathrm{I}} + 0.388\sigma_R - 0.287\upsilon + 0.143\pi - 0.451$	0.997
	$\sigma_{\mathrm{I}}, \sigma_R, \upsilon$, MR, π	$0.256\sigma_{\mathrm{I}} + 0.388\sigma_R - 0.262\upsilon - 0.003\ \mathrm{MR} + 0.145\pi - 0.446$	0.999

and molar refractivity parameters are important in the nitration of phenols.

$$\log k = 0.176\,\sigma_{\mathrm{I}} + 0.580\sigma_R - 0.456\upsilon + 0.017\,\mathrm{MR} + 0.270\,\pi - 0.673;\ R^2 = 0.982 \tag{37}$$

(when Charton's polar, resonance, steric, hydrophobicity, and molar refractivity parameters are considered) Detailed Charton's analysis at different temperatures in a set of solvents is given in Table IX and X (for other tables, see Tables AVII–AX in the Appendix). It is of interest to note that when log k_{exp} values are correlated with log k_{cal} a perfect linearity is obtained with the correlation coefficient of unity, as can be seen from the data given in Tables XI and XII (for other tables, see Tables AXI–AXIII in the Appendix).

CONCLUSIONS

In summary, in the present study, we have developed an acid free protocol for nitration of phenols TBN under conventional conditions. The authors have also taken up a detailed colorimetric kinetic study of nitration of phenols using TBN in different solvents to gain an insight into mechanistic aspects. The reaction followed second-order kinetics with first-order dependence on [TBN] and [phenol]. All the TBN-mediated nitration of different phenols reactions have been studied in different solvent media at four to five temperatures in 20°C range (30–50°C). The rate of nitration increased with an increase in temperature in different the solvent media (MeCN, DCE, CCl_4, DMF, and toluene). Rates of nitration (log k) could not fit into either Amis or Kirkwood plots [log k' versus ($1/D$) or [$(D - 1)/(2D + 1)$]]. However, the trends were better explained by the basic form of Koppel and Palm's MLSER, to explain the multiple interacting effects of the solvent on the reactivity of substrates in the nitration of phenols:

$$\log k = p_1\pi* + p_2\alpha + p_3\beta + p_4\delta + \text{constant} \tag{38}$$

where π* is solvent dipolarity/polarizability, α is HBD, β is the HBA basicity parameter, δ is the Hildebrand solubility parameter, and p_1, p_2, p_3, and p_4 are corresponding coefficients. MLRA of the kinetic data pertains to the nitration of phenols in various solvents furnished the parameters p_1, p_2, p_3, and p_4. Detailed stepwise analysis indicated that none of the Koppel and Palm's basic solvent parameters (π*, α, β, and δ) alone are responsible for the solvation of the transition state during nitration of phenols. But the regression analysis excellent linearity is obtained with the correlation coefficient of unity ($R^2 = 1.00$) when the entire basic parameters are used.

$$\log k = 0.829\pi* + 2.124\alpha + 1.061\beta - 0.263\delta + 1.106;\ R^2 = 1.00$$

Table X Charton Analysis: $\log k = a_1\sigma_\mathrm{I} + a_2\sigma_\mathrm{R} + a_3\,\upsilon + a_4\,\mathrm{MR} + a_5\pi + \mathrm{Constant}$

Solvent	Temperature (K)	a_1	a_2	a_3	a_4	a_5	R^2
MeCN	303	0.176	0.580	–0.456	+0.017	0.270	0.982
	313	0.265	0.373	–0.206	–0.005	0.197	0.984
	323	0.256	0.388	–0.262	–0.003	0.145	0.999
DMF	303	–1.714	–0.129	–0.008	+0.089	–1.009	0.989
	313	–1.551	–0.339	–0.168	0.083	–0.888	0.991
	323	–1.058	–0.635	–0.257	–0.062	–0.604	0.992
Toluene	303	0.150	–0.672	–0.162	–0.018	0.091	0.985
	313	0.064	–0.500	–0.112	–0.023	0.133	0.978
	323	0.062	–0.498	–0.141	–0.028	0.189	0.985
CCl_4	303	0.470	–0.714	0.488	–0.005	–0.174	0.999
	313	0.408	–0.508	0.166	–0.010	–0.062	0.998
	323	0.284	–0.320	0.123	–0.008	–0.025	0.996
DCE	303	–0.015	0.541	1.275	–0.062	0.238	0.999
	313	0.002	0.660	1.009	–0.055	0.214	0.999
	323	0.019	0.707	0.945	–0.048	0.205	1.00

Table XI $\log k_\mathrm{exp}$ versus $\log k_\mathrm{cal}$ for MeCN

	Temperature (K)					
	303		313		323	
Substrate	$\log k_\mathrm{exp}$	$\log k_\mathrm{cal}$	$\log k_\mathrm{exp}$	$\log k_\mathrm{cal}$	$\log k_\mathrm{exp}$	$\log k_\mathrm{cal}$
Phenol	–0.6676	0.01751	–0.5969	–0.0051	–0.451	–0.00309
o-Cl	–0.6162	0.01997	–0.5114	0.05118	–0.4547	–0.01132
Catechol	–1.1739	–0.48605	–0.8996	–0.3047	–0.7399	–0.29114
o-Cresol	–0.7328	–0.07407	–0.6635	–0.0867	–0.5817	–0.13523
o-Br	–0.6517	0.0714	–0.5719	0.04804	–0.4789	–0.02168
o-OMe	–0.8894	–0.23185	–0.7799	–0.2025	–0.6615	–0.21467
o-NO_2	–0.5751	0.09132	–0.5186	0.06414	–0.3778	0.07022
Equation	$y = 0.9829x + 0.6606$		$y = 0.9864x + 0.5778$		$y = 1.0019x + 0.4494$	
R^2	$R^2 = 0.9821$		$R^2 = 0.9842$		$R^2 = 0.9989$	

This observation probably strengthens our view that cumulative contributions of basic solvent parameters might be responsible for solvation. The coefficients corresponding to different variables (π^*, α, β, and δ) further reveal that apart from solvent dipolarity/polarizability (π^*), HBD and HBA properties (α, β), and Hildebrand solubility parameter (δ) are contributing substantially for the solvation of transition state. The positive magnitudes of coefficients p_2 and p_3 ($+2.124\alpha$, $+1.061\beta$) may probably indicate the favorable attack of the nitronium ion at electron-rich benzene ring to afford nitro derivative.

On the other hand, the solvent effects were explained by Kamlet and Taft's MLSER as shown below:

$$\log k = m_1\varphi_1 + m_2\varphi_2 + m_3\varphi_3 + m_4\varphi_4 + \text{constant}$$

where ϕ_1 is the dielectric constant function, $(D - 1)/(2D + 1)$; ϕ_2 is the viscosity function, 1/viscosity; ϕ_3 is the refractive index function, $(\eta^2 - 1)/(\eta^2 + 2)$; ϕ_4 is the density, whereas m_1, m_2, m_3, and m_4 are corresponding coefficients. Furthermore, ϕ_1 and ϕ_3 indicate equilibrium solvent parameters whereas ϕ_2 (reciprocal of viscosity) and ϕ_4 (density) indicate frictional solvent properties. Statistical analysis using "multiple linear regression technique" afforded parameters under different conditions. A perusal of the computed results (using Eq. (17)), which are given in Table VII, clearly show that when all solvent parameters (ϕ_1, ϕ_2, ϕ_3, and ϕ_4) are used in the regression analysis excellent linearity is obtained with the correlation coefficient of unity ($R^2 = 1.00$). However, the regression analysis afforded poor correlation coefficients ($R^2 < 0.900$ or even lesser than this value) when any one of the solvent parameters is excluded from the analysis. This

Table XII $\log k_{\text{exp}}$ versus $\log k_{\text{cal}}$ for DMF

	Temperature (K)					
	303		313		323	
Substrate	$\log k_{\text{exp}}$	$\log k_{\text{cal}}$	$\log k_{\text{exp}}$	$\log k_{\text{cal}}$	$\log k_{\text{exp}}$	$\log k_{\text{cal}}$
Phenol	–0.6234	0.09167	–0.4921	0.08549	–0.4012	0.06386
o-Cl	–1.6021	–0.98894	–1.3468	–0.87483	–0.9706	–0.56871
Catechol	–0.2233	0.49806	–0.063	0.50814	0.02407	0.49288
o-Cresol	–0.6615	–0.00132	–0.5258	0.00593	–0.4168	0.01387
o-Br	–1.6576	–0.86294	–1.3872	–0.76404	–1.0132	–0.49985
o-OMe	–0.3747	0.28321	–0.1818	0.3341	–0.0405	0.38854
o-NO_2	–0.8996	–0.22389	–0.7747	–0.25828	–0.6882	–0.24746
Equation	$y = 0.9889x + 0.6816$		$y = 1.0011x + 0.5447$		$y = 0.9921x + 0.446$	
R^2	$R^2 = 0.9893$		$R^2 = 0.9909$		$R^2 = 0.9924$	

observation probably strengthens our view once again cumulative contributions of basic solvent parameters might be responsible for solvation. In addition to this, the observed results may also indicate the importance of equilibrium as well as frictional solvent effects and solvent–solute interactions for solvation of transition state during nitration of phenols.

A closer look into the kinetic data pertaining to the TBN nitration of phenols revealed that the reaction is sensitive to the structural variation of phenol. Reaction rates accelerated with the introduction of electron-donating groups and retarded with electron-withdrawing groups. Accordingly, the reactivity of structurally different phenols was found to follow the sequence: *p*-OH > *p*-MeO > p-Me > H > *m*-Me > *p*-Cl > *p*-Br > *m*-Cl > *p*-NO_2 > *m*-OH. The results are interpreted by Hammett's theory of linear free energy relationship. The reaction constant (Hammett's ρ) is a measure of the sensitivity of the reaction toward the electronic effects of the substituent. The rho (ρ) values obtained from the present experiments are fairly large negative values ($\rho < 0$), indicating attack of an electrophile on the aromatic ring. An increase in temperature decreases the reaction constant (ρ) values. According to Exner, ρ values for a given reaction are influenced by the temperature according to the following relation:

$$\rho = A[1 - \beta/T]$$

Obtained "isokinetic temperature (β)" values are in the range of 225–290, as can be seen from Table VIII. These values are far below the experimental temperature range (303–323 K), indicating that the entropy factors are probably more important in controlling the reaction. This point can be seen from the negative entropy values and linearity of MLRA.

Ortho Effect: In the present study, rate constants for TBN nitration of ortho-substituted phenols could not fit into Taft's plots of $\log(k/k_{\text{CH3}})$ versus (σ^*) or, $\log(k/k_{\text{CH3}})$ versus E_s or combined did not give good correlations. When the regression analysis was tried with Charton's polar, resonance, steric, and hydrophobicity parameters the correlation gradually increased from Taft's analysis to Charton analysis. Very good linearity was obtained when Charton's polar, resonance, steric, hydrophobicity, and molar refractivity parameters are considered.

$$\log k = \mathrm{a}_1\sigma_{\mathrm{I}} + a_2\sigma_R + a_3\upsilon + a_4\,\mathrm{MR} + a_5\pi + \text{constant}$$

where σ_{I} is the inductive constant of substituent, σ_R is the mesomeric/resonance constant; υ is the steric substituent constant, and $a_{1,}$ $a_{2,}$ and a_3 are corresponding coefficients. For instance, MLRA of the kinetic data pertains to the nitration of phenols in acetonitrile at 303 K depicted a very good linear relationship when Charton's polar, resonance, steric, hydrophobicity, and molar refractivity parameters are considered, as shown in the following equation:

$$\log k = 0.176\,\sigma_{\mathrm{I}} + 0.580\,\sigma_R - 0.456\upsilon + 0.017\,\mathrm{MR} + 0.270\,\pi - 0.673;\ R^2 = 0.982$$

It is of interest to note that when $\log k_{\text{exp}}$ values are correlated with $\log k_{\text{cal}}$ the perfect linearity is obtained with correlation coefficient of unity, as can be seen from the data given in Tables XI–XII.

APPENDIX

Table AI MLSER for Ortho-Substituted Phenols at 303 K

Substrate	p_1	p_2	p_3	p_4	Constant	R^2	Remark
o-Cl phenol	0.194	1.361	–2.00	0.036	–0.824	1	Considering all parameters
	0.275	1.622	–1.88	–	–0.547	1	Parameter δ excluded
	1.251	5.254	–	–0.500	3.393	0.908	Parameter β excluded
	–0.14	–	–2.51	0.191	–2.031	0.992	Parameter α excluded
	0.264	–	–	–0.236	1.530	0.455	Parameters α and β excluded
Catechol	–1.39	–4.09	0.889	0.066	–0.413	1	Considering all parameters
	–1.24	–3.61	1.108	–	0.099	0.998	Parameter δ excluded
	–1.86	–5.82	–	0.304	–2.285	0.974	Parameter β excluded
	–0.37	–	2.426	–0.400	3.217	0.892	Parameter α excluded
	–0.77	–	–	0.012	–0.220	0.168	Parameters α and β excluded
o-Cresol	0.326	–2.24	–1.16	0.193	–2.490	1	Considering all parameters
	0.767	–0.82	–0.52	–	–0.990	0.903	Parameter δ excluded
	0.940	0.026	–	–0.118	–0.040	0.717	Parameter β excluded
	0.882	–	–0.32	–0.062	–0.508	0.798	Parameter α excluded
	0.935	–	–	–0.117	–0.049	0.717	Parameters α and β excluded
o-Br phenol	0.262	1.576	–1.95	0.009	–0.648	1	Considering all parameters
	0.283	1.642	–1.92	–	–0.579	1	Parameter δ excluded
	1.294	5.375	–	–0.513	3.467	0.916	Parameter β excluded
	–0.13	–	–2.54	0.189	–2.046	0.989	Parameter α excluded
	0.285	–	–	–0.244	1.561	0.460	Parameters α and β excluded
o-NO_2 phenol	–1.06	–1.25	–1.33	0.345	–3.233	1	Considering all parameters
	–0.27	1.274	–0.19	–	–0.554	0.680	Parameter δ excluded
	–0.35	1.34	–	–0.012	–0.424	0.614	Parameter β excluded
	–0.75	–	–0.87	0.203	–2.125	0.935	Parameter α excluded
	–0.61	–	–	0.056	–0.901	0.334	Parameters α and β excluded
o-OMe phenol	–1.14	–1.40	1.05	–0.016	0.097	1	Considering all parameters
	–1.18	–1.52	1.00	–	–0.025	1	Parameter δ excluded
	–0.70	–3.45	–	0.265	–2.118	0.923	Parameter β excluded
	–0.79	–	1.581	–0.018	1.345	0.973	Parameter α excluded
	–1.050	–	–	0.092	–0.894	0.327	Parameters α and β excluded

Table AII MLSER for Meta-Substituted Phenols at 303 K

Substrate	p_1	p_2	p_3	p_4	Constant	R^2	Remark
Resorcinol	–2.16	–9.41	–1.06	0.845	–7.50	1	Considering all parameters
	–0.230	–3.23	11.7	–	–0.933	0.833	Parameter δ excluded
	–0.1600	–7.354	–	0.561	–5.262	0.979	Parameter β excluded
	0.184	–	2.475	–0.28	0.852	0.676	Parameter α excluded
	–0.219	–	–	0.192	–2.654	0.247	Parameters α and β excluded
m-Cl phenol	1.030	1.433	–0.970	–0.098	–0.523	1	Considering all parameters
	0.805	0.712	–1.297	–	–1.288	0.992	Parameter δ excluded
	1.542	3.319	–	–0.358	1.520	0.939	Parameter β excluded
	0.673	–	–1.508	0.065	–1.793	0.974	Parameter α excluded
	0.919	–	–	–0.191	0.343	0.429	Parameters α and β excluded
m-Cresol	0.592	2.589	0.807	–0.230	0.915	1	Considering all parameters
	0.067	0.908	0.045	–	–0.870	0.563	Parameter δ excluded
	0.166	1.020	–	–0.014	–0.786	0.664	Parameter β excluded
	–0.052	–	–0.165	0.065	–1.381	0.33	Parameter α excluded
	–0.025	–	–	0.037	–1.147	0.281	Parameters α and β excluded

Table AIII Multivariate Linear Solvent Energy Relationship at 308 K

Substrate	p_1	p_2	p_3	p_4	Constant	R^2
Phenol	0.651	1.557	0.989	–0.247	1.204	1
p-Cresol	0.487	1.841	1.555	–0.302	1.821	1
p-Cl phenol	0.659	0.141	–0.473	–0.077	–0.338	1
p-Br phenol	0.567	0.212	–0.366	–0.083	–0.234	1
Quinol	–0.077	0.707	1.937	–0.199	1.229	1
p-NO_2 phenol	0.942	0.000	–2.531	0.111	–2.249	1
p- OMe phenol	0.089	1.126	2.096	–0.245	1.501	1

Table AIV Multivariate Linear Solvent Energy Relationship at 313 K

Substrate	p_1	p_2	p_3	p_4	Constant	R^2
Phenol	0.518	0.830	0.625	–0.176	0.757	1
p-Cresol	0.279	1.185	1.201	–0.218	1.283	1
p-Cl phenol	0.450	0.515	–0.507	–0.308	–0.466	1
p-Br phenol	0.468	0.795	–0.382	–0.063	–0.255	1
Quinol	–0.105	0.658	1.817	–0.185	1.202	1
p-OMe phenol	0.066	0.731	1.810	–0.209	1.323	1
p-NO_2 phenol	0.741	0.000	–2.859	0.176	–2.615	1
o-Cl phenol	0.314	1.412	–1.584	–0.025	–0.229	1
Catechol	–1.143	–3.276	0.919	0.057	–0.379	1
o-Br phenol	0.308	1.327	–1.566	–0.34	–0.164	1
o-OMe phenol	–0.987	–1.766	1.026	0.004	–0.066	1
o-NO_2 phenol	–0.880	–1.915	–1.557	0.358	–3.278	1
o-Cresol	0.496	–1.749	–0.728	0.073	–1.343	1
Resorcinol	–2.919	–10.774	–2.237	1.138	–9.483	1
m-Cl phenol	0.725	0.800	–1.057	–0.030	–0.704	1
m-Cresol	0.116	0.435	0.044	–0.038	–0.271	1

Table AV Multivariate Linear Solvent Energy Relationship at 318 K

Substrate	p_1	p_2	p_3	p_4	Constant	R^2
Phenol	0.374	0.757	0.603	–0.161	0.776	1
p-Cresol	0.314	1.132	1.152	–0.221	1.358	1
p-Cl phenol	0.353	0.238	–0.481	–0.016	–0.544	1
p-Br phenol	0.482	0.779	–0.213	–0.085	0.006	1
Quinol	–0.256	0.150	1.621	–0.123	0.797	1
p-NO_2 phenol	0.586	0.000	–2.758	0.192	–2.584	1
p- OMe phenol	0.029	0.019	1.509	–0.150	0.896	1

Table AVI Multivariate Linear Solvent Energy Relationship at 323 K

Substrate	p_1	p_2	p_3	p_4	Constant	R^2
Phenol	0.347	1.030	0.648	–0.176	0.977	1
p-Cresol	0.292	1.179	1.084	–0.215	1.372	1
p-Cl phenol	0.386	0.468	–0.447	–0.031	–0.350	1
p-Br phenol	0.379	0.698	–0.344	–0.045	–0.233	1
Quinol	–0.306	–0.103	1.483	–0.096	0.633	1
p-OMe phenol	–0.064	–0.451	1.234	–0.086	0.421	1
p-NO_2 phenol	0.415	0.000	–2.897	0.235	–2.813	1
o-Cl phenol	0.272	0.583	–1.143	–0.25	–0.113	1
Catechol	–0.963	–2.488	1.090	0.010	–0.001	1
o-Cresol	0.331	–1.837	–0.640	0.068	–1.089	1
o-Br phenol	0.218	0.425	–1.268	–0.001	–0.322	1
o-OMe phenol	–0.871	–1.555	1.168	–0.021	0.177	1
o-NO_2 phenol	–0.955	–2.075	–1.787	0.410	–3.593	1
Resorcinol	–3.071	–10.370	–2.241	1.127	–9.161	1
m-Cl phenol	0.563	1.061	–0.683	–0.059	–0.224	1
m-Cresol	–0.044	0.496	0.244	–0.046	0.026	1

Table AVII Charton Analysis for DMF

Temperature (K)	Parameter	Equation	R^2
303	σ^*	$-1.4232\sigma^* + 0.7272$	0.2903
	E_s	$-0.422E_s + 0.6343$	0.0902
	σ^*, E_s	$-0.291\sigma^* + 0.211E_s - 0.505$	0.325
	$\sigma_I, \sigma_R, \upsilon$	$-0.354\sigma_I - 1.176\sigma_R - 1.712\upsilon - 0.286$	0.635
	$\sigma_I, \sigma_R, \upsilon$, MR	$-0.583\sigma_I - 1.214\sigma_R - 2.247\upsilon + 0.062\text{MR} - 0.365$	0.664
	$\sigma_I, \sigma_R, \upsilon, \pi$	$-1.329\sigma_I - 0.134\sigma_R + 0.560\upsilon - 0.955\pi - 0.560$	0.932
	$\sigma_I, \sigma_R, \upsilon$, MR, π	$-1.714\sigma_I - 0.129\sigma_R - 0.08\upsilon + 0.089\text{MR} - 1.009\pi - 0.690$	0.989
313	σ^*	$-1.5482\sigma^* + 0.9004$	0.2931
	E_s	$-0.5166E_s + 0.6465$	0.1153
	σ^*, E_s	$-0.244\sigma^* + 0.134E_s - 0.337$	0.309
	$\sigma_I, \sigma_R, \upsilon$	$-0.296\sigma_I - 1.258\sigma_R - 1.560\upsilon - 0.195$	0.665
	$\sigma_I, \sigma_R, \upsilon$, MR	$-0.516\sigma_I - 1.294\sigma_R - 2.075\upsilon + 0.059\text{ MR} - 0.271$	0.695
	$\sigma_I, \sigma_R, \upsilon, \pi$	$-1.150\sigma_I - 0.345\sigma_R + 0.432\upsilon - 0.837\pi - 0.436$	0.932
	$\sigma_I, \sigma_R, \upsilon$, MR, π	$-1.551\sigma_I - 0.339\sigma_R - 0.168\upsilon + 0.083\text{MR} - 0.888\pi - 0.557$	0.991
323	σ^*	$-2.0097\sigma^* + 0.949$	0.3076
	E_s	$-0.8372E_s + 0.5792$	0.1887
	σ^*, $\mathrm{E_s}$	$-0.151\sigma^* - 0.005E_s - 0.201$	0.308
	$\sigma_I, \sigma_R, \upsilon$	$-0.212\sigma_I - 1.257\sigma_R - 1.157\upsilon - 0.197$	0.743
	$\sigma_I, \sigma_R, \upsilon$, MR	$-0.382\sigma_I - 1.285\sigma_R - 1.554\upsilon + 0.046\text{MR} - 0.255$	0.773
	$\sigma_I, \sigma_R, \upsilon, \pi$	$-0.790\sigma_I - 0.639\sigma_R + 0.190\upsilon - 0.566\pi - 0.359$	0.939
	$\sigma_I, \sigma_R, \upsilon$, MR, π	$-1.058\sigma_I - 0.635\sigma_R - 0.257\upsilon - 0.062\text{MR} - 0.604\pi - 0.450$	0.992

Table AVIII Charton Analysis for Toluene

Temperature (K)	Parameter	Equation	R^2
303	σ^*	$-4.4349\sigma^* + 0.9393$	0.1455
	E_s	$-4.0926E_s - 1.6674$	0.4378
	σ^*, E_s	$0.029\sigma^* - 0.149E_s - 0.559$	0.482
	$\sigma_I, \sigma_R, \upsilon$	$-0.008\sigma_I - 0.583\sigma_R - 0.097\upsilon - 0.709$	0.900
	$\sigma_I, \sigma_R, \upsilon$, MR	$0.048\sigma_I - 0.574\sigma_R - 0.034\upsilon - 0.015\text{MR} - 0.690$	0.933
	$\sigma_I, \sigma_R, \upsilon, \pi$	$0.074\sigma_I - 0.671\sigma_R - 0.289\upsilon + 0.081\pi - 0.686$	0.941
	$\sigma_I, \sigma_R, \upsilon$, MR, π	$0.150\sigma_I - 0.672\sigma_R - 0.162\upsilon - 0.018\ \text{MR} + 0.091\pi - 0.660$	0.985
313	σ^*	$-8.0586\sigma^* - 2.0415$	0.3454
	E_s	$-5.6202E_s - 1.7891$	0.5937
	σ^*, E_s	$0.002\sigma^* - 0.108E_s - 0.391$	0.594
	$\sigma_I, \sigma_R, \upsilon$	$-0.158\sigma_I - 0.369\sigma_R + 0.003\upsilon - 0.513$	0.747
	$\sigma_I, \sigma_R, \upsilon$, MR	$-0.085\sigma_I - 0.357\sigma_R + 0.174\upsilon - 0.020\text{MR} - 0.488$	0.826
	$\sigma_I, \sigma_R, \upsilon, \pi$	$-0.037\sigma_I - 0.499\sigma_R - 0.280\upsilon + 0.119\pi - 0.479$	0.870
	$\sigma_I, \sigma_R, \upsilon$, MR, π	$0.064\sigma_I - 0.500\sigma_R - 0.112\upsilon - 0.023\text{MR} + 0.133\pi - 0.445$	0.978
323	σ^*	$-7.7157\ \sigma^* - 1.091$	0.3811
	E_s	$-5.1048E_s - 0.9696$	0.5895
	σ^*, E_s	$-0.004\sigma^* - 0.109\ E_s - 0.268$	0.591
	$\sigma_I, \sigma_R, \upsilon$	$-0.235\sigma_I - 0.309\sigma_R + 0.065\upsilon - 0.395$	0.640
	$\sigma_I, \sigma_R, \upsilon$, MR	$-0.150\sigma_I - 0.295\sigma_R + 0.265\upsilon - 0.023\text{MR} - 0.365$	0.729
	$\sigma_I, \sigma_R, \upsilon, \pi$	$-0.060\sigma_I - 0.496\sigma_R - 0.344\upsilon + 0.172\pi - 0.345$	0.855
	$\sigma_I, \sigma_R, \upsilon$, MR, π	$0.062\sigma_I - 0.498\sigma_R - 0.141\upsilon - 0.028\text{MR} + 0.189\pi - 0.304$	0.985

Table AIX Charton Analysis for CCl_4

Temperature (K)	Parameter	Equation	R^2
303	σ^*	$2.5467\sigma^* + 3.3238$	0.1581
	E_s	$-0.4041E_s + 0.7815$	0.0141
	σ^*, E_s	$0.192\ \sigma^* - 0.316E_s - 0.598$	0.618
	$\sigma_I, \sigma_R, \upsilon$	$0.628\sigma_I - 0.907\sigma_{\mathrm{R}} + 0.028\upsilon - 0.884$	0.938
	$\sigma_I, \sigma_R, \upsilon$, MR	$0.665\sigma_I - 0.901\sigma_R + 0.115\upsilon - 0.010\text{MR} - 0.871$	0.942
	$\sigma_I, \sigma_R, \upsilon, \pi$	$0.447\sigma_I - 0.713\sigma_R + 0.450\upsilon - 0.177\pi - 0.935$	0.998
	$\sigma_I, \sigma_R, \upsilon$, MR, π	$0.470\sigma_I - 0.714\sigma_R + 0.488\upsilon - 0.005\text{MR} - 0.174\pi - 0.927$	0.999
313	σ^*	$4.351\sigma^* + 3.7374$	0.1788
	E_s	$-0.2917E_s + 0.8791$	0.0028
	σ^*, E_s	$0.113\sigma^* - 0.174E_s - 0.456$	0.542
	$\sigma_I, \sigma_R, \upsilon$	$0.434\sigma_I - 0.581\sigma_R - 0.067\upsilon - 0.608$	0.964
	$\sigma_I, \sigma_R, \upsilon$, MR	$0.477\sigma_I - 0.574\sigma_R + 0.034\upsilon - 0.012\text{MR} - 0.593$	0.979
	$\sigma_I, \sigma_R, \upsilon, \pi$	$0.365\sigma_I - 0.508\sigma_R + 0.094\upsilon - 0.068\pi - 0.627$	0.986
	$\sigma_I, \sigma_R, \upsilon$, MR, π	$0.408\sigma_I - 0.508\sigma_R + 0.166\upsilon - 0.010\text{MR} - 0.062\pi - 0.613$	0.998
323	σ^*	$-7.539\sigma^* + 5.2453$	0.2184
	E_s	$-0.2936E_s + 0.9094$	0.0012
	σ^*, E_s	$0.077\sigma^* - 0.116\ E_s - 0.338$	0.615
	$\sigma_I, \sigma_R, \upsilon$	$0.279\sigma_I - 0.352\sigma_R - 0.009\upsilon - 0.441$	0.966
	$\sigma_I, \sigma_R, \upsilon$, M.R	$0..312\sigma_I - 0.347\sigma_R + 0.069\upsilon - 0.009\text{MR} - 0.429$	0.989
	$\sigma_I, \sigma_R, \upsilon, \pi$	$0.248\sigma_I - 0.319\sigma_R + 0.064\upsilon - 0.030\pi - 0.450$	0.977
	$\sigma_I, \sigma_R, \upsilon$, MR, π	$0.284\sigma_I - 0.320\sigma_R + 0.123\upsilon - 0.008\text{MR} - 0.025\pi - 0.438$	0.996

Table AX Charton Analysis for DCE

Temperature (K)	Parameter	Equation	R^2
303	σ^*	$-0.4559\sigma^* + 0.2423$	0.0076
	E_s	$-0.3235E_s + 0.7951$	0.0135
	σ^*, E_s	$0.085\sigma^* - 0.166E_s - 0.630$	0.092
	$\sigma_I, \sigma_R, \upsilon$	$-0.490\sigma_I + 0.764\sigma_R + 1.301\upsilon - 0.868$	0.836
	$\sigma_I, \sigma_R, \upsilon$, MR	$-0.282\sigma_I + 0.797\sigma_R + 1.786\upsilon - 0.056\mathrm{MR} - 0.797$	0.928
	$\sigma_I, \sigma_R, \upsilon, \pi$	$-0.286\sigma_I + 0.545\sigma_R + 0.825\upsilon + 0.200\pi - 0.811$	0.887
	$\sigma_I, \sigma_R, \upsilon$, MR, π	$-0.015\sigma_I + 0.541\sigma_R + 1.275\upsilon - 0.062\mathrm{MR} + 0.238\pi - 0.720$	0.999
313	σ^*	$0.6839\sigma^* + 2.2791$	0.0134
	E_s	$0.0716E_s + 1.0324$	0.0005
	σ^*, E_s	$0.042\sigma^* - 0.054E_s - 0.501$	0.025
	$\sigma_I, \sigma_R, \upsilon$	$-0.421\sigma_I + 0.860\sigma_R + 1.039\upsilon - 0.613$	0.835
	$\sigma_I, \sigma_R, \upsilon$, MR	$-0.237\sigma_I + 0.890\sigma_R + 1.468\upsilon - 0.049\mathrm{MR} - 0.550$	0.926
	$\sigma_I, \sigma_R, \upsilon, \pi$	$-0.237\sigma_I + 0.663\sigma_R + 0.611\upsilon + 0.180\pi - 0.562$	0.888
	$\sigma_I, \sigma_R, \upsilon$, MR, π	$0.002\sigma_I + 0.660\sigma_R + 1.009\upsilon - 0.055\mathrm{MR} + 0.214\pi - 0.481$	0.999
323	σ^*	$1.0313\sigma^* + 2.3521$	0.0303
	E_s	$0.2899E_s + 1.11$	0.0085
	σ^*, E_s	$0.044\sigma^* - 0.022E_s - 0.444$	0.044
	$\sigma_I, \sigma_R, \upsilon$	$-0.369\sigma_I + 0.902\sigma_R + 1.017\upsilon - 0.524$	0.864
	$\sigma_I, \sigma_R, \upsilon$, MR	$-0.211\sigma_I + 0.928\sigma_R + 1.386\upsilon - 0.043\mathrm{MR} - 0.470$	0.932
	$\sigma_I, \sigma_R, \upsilon, \pi$	$-0.190\sigma_I + 0.710\sigma_R + 0.598\upsilon + 0.176\pi - 0.474$	0.915
	$\sigma_I, \sigma_R, \upsilon$, MR, π	$0.019\sigma_I + 0.707\sigma_R + 0.945\upsilon - 0.048\mathrm{MR} + 0.205\pi - 0.403$	1.00

Table AXI log k_{exp} versus log k_{cal} for Toluene

	Temperature (K)					
	303		313		323	
Substrate	log k_{exp}	log k_{cal}	log k_{exp}	log k_{cal}	log k_{exp}	log k_{cal}
Phenol	–0.6716	–0.01854	–0.4622	–0.02369	–0.327	–0.02884
o-Cl	–0.6216	0.05693	–0.4547	0.01358	–0.3188	0.00596
Catechol	–0.4789	0.17207	–0.3904	0.04678	–0.3125	–0.01569
o-Cresol	–0.7212	–0.05512	–0.5072	–0.05191	–0.3768	–0.06404
o-Br	–0.6421	–0.01336	–0.4737	–0.0545	–0.3497	–0.07079
o-OMe	–0.5452	0.12094	–0.4535	0.00329	–0.3625	–0.049
o-NO_2	–0.8794	–0.21796	–0.7305	–0.27912	–0.6517	–0.34275
Equation	$y = 0.9871x + 0.6495$		$y = 0.9752x + 0.4344$		$y = 0.9836x + 0.2985$	
R^2	$R^2 = 0.9849$		$R^2 = 0.9779$		$R^2 = 0.9845$	

Table AXII log k_{exp} versus log k_{cal} for CCl_4

	Temperature (K)					
	303		313		323	
Substrate	log k_{exp}	log k_{cal}	log k_{exp}	log k_{cal}	log k_{exp}	log k_{cal}
Phenol	–0.9355	–0.00515	–0.6198	–0.0103	–0.4437	–0.00824
o-Cl	–0.4609	0.45943	–0.3556	0.2661	–0.2573	0.1899
Catechol	–0.2321	0.69955	–0.209	0.39984	–0.1844	0.25079
o-Cresol	–0.7282	0.19739	–0.5751	0.04074	–0.4101	0.03216
o-Br	–0.4976	0.4442	–0.3726	0.22658	–0.2668	0.16357
o-OMe	–0.3595	0.56659	–0.3107	0.30582	–0.2503	0.1929
o-NO_2	–0.5467	0.38112	–0.4237	0.19086	–0.3134	0.12777
Equation	$y = 1.0008x + 0.9295$		$y = 0.9978x + 0.6114$		$y = 0.9993x + 0.439$	
R^2	$R^2 = 0.9992$		$R^2 = 0.9975$		$R^2 = 0.9961$	

Table AXIII log k_{exp} versus log k_{cal} for DCE

	Temperature (K)					
	303		313		323	
Substrate	log k_{exp}	log k_{cal}	log k_{exp}	log k_{cal}	log k_{exp}	log k_{cal}
Phenol	–0.7878	–0.06386	–0.5406	–0.05665	–0.4547	–0.04944
o-Cl	–0.3188	0.39209	–0.2168	0.25736	–0.1409	0.25734
Catechol	–0.8962	–0.17025	–0.752	–0.26711	–0.684	–0.2777
o-Cresol	–0.341	0.3764	–0.2314	0.24787	–0.1593	0.24214
o-Br	–0.3487	0.38971	–0.2472	0.24677	–0.1518	0.25955
o-OMe	–0.983	–0.26497	–0.8297	–0.35055	–0.7352	–0.33347
o-NO_2	–0.7258	–0.00531	–0.4921	–0.01127	–0.3645	0.03847
Equation	$y = 1.0001x + 0.7222$		$y = 1.0003x + 0.4825$		$y = 0.9992x + 0.4036$	
R^2	$R^2 = 0.9991$		$R^2 = 0.9994$		$R^2 = 0.9997$	

BIBLIOGRAPHY

1. (a) Olah, G. A.; Malhotra, R.; Narang, S. C. Organic Nitro Chemistry Series- “Nitration Methods and Mechanisms” VCH: New York, 1989; (b) Hoggett, J. G.; Monodie, R. B.; Penton, J. R.; Schofield, K. “Nitration and aromatic Reactivity”; Cambridge University: London, 1971.
2. Ono, N. The Nitro Group in Organic Synthesis; Wiley-VCH: New York, 2001.
3. Sykes, P. A Guide book to Mechanism in Organic Chemistry, 6th ed.; Longman Scientific & Technical: London, 1967; p. 130.
4. Olah, G. A.; Stephen J. Kuhn Org Synth Coll 1973, 5, 480; 1967, 47, 56.
5. Hughes, E. D.; Ingold, C. K.; Reed, R. I. Nature 1946, 158, 448.
6. Halberstadt, E. S.; Hughes, E. D.; Ingold, C. K. Nature 1946, 158, 514.
7. Halberstadt, E. S.; Hughes, E. D.; Ingold, C. K. J Chem Soc 1950, 2441.
8. Kecki, Z. Tetrahedron 1961, 12, 23.
9. Kulkarni, A. A. Beilstein J Org Chem 2014, 10, 405.
10. Prakash, S.; Mathew, T. Angew Chem, Int 2010, 49, 1726.
11. Kogelbauer, A.; Vassena, D.; Prins, R.; Armor, J. N. Catal Today 2000, 55, 151.
12. Riego, J. M.; Sedin, Z.; Zaldivar, J. M.; Marziano, N. C.; Tortato, C. Tetrahedron Lett 1996, 37, 513.
13. Peng, X.; Suzuki, H.; LU, C. Tetrahedron Lett 2001, 42, 4357.
14. Dagade, S. P.; Waghmode, S. B.; Kadam, V. S.; Dongare, M. K. Appl Catal, A 2002, 49, 226.
15. Radoslaw, R. B.; Andrew, J. S. Tetrahedron Lett 2001, 42, 6767.
16. Iranpoor, N.; Firouzabadi, H.; Heydari, R. Phosphorus, Sulfur Silicon 2003, 178, 1027.

17. Rodrigues, J. A. R.; Oliveira Filho, A. P.; Moran, P. J. S.; Custodio, R. (a) Tetrahedron 1999, 55, 6733; (b) Synth. Commun. 1999, 29, 2169.
18. (a) Delaude, L.; Laszlo, P.; Smith, K. Acc Chem Res 1993, 26, 607; (b) Laszlo, P. Acc Chem Res 1986, 19, 121.
19. (a) Zolfigol, M. A.; Iranpoor, N.; Firouzabadi, H. Orient J Chem 1998, 14, 369; (b) Firouzabadi, H.; Iranpoor, N.; Zolfigol, M. A. Iran J Chem Chem Eng 1997, 16, 48.
20. Jean-Luc, G.; Nicole, C.; Philippe, C.; Jean-Pierre, C. Bioorg Med Chem Lett 1996, 6, 431.
21. Messere, A.; Gentili, A.; Garella, I.; Temussic, F.; Di Blasio, B.; Fiorentino, A. Synth Commun 2004, 34, 3317.
22. Ramgopal, S.; Ramesh, K.; Maasi Reddy, N.; Chakradhar, A.; Rajanna, K. C. Tetrahedron Lett 2007, 48, 4043
23. Koley, D.; Colón, O. C.; Savinov, S. N. Org Lett 2009, 11, 4172.
24. Kilpatrick, B.; Arns, S. Chem Commun 2013, 49, 514.
25. Satish Kumar, M.; Rajanna, K. C.; Rajendar Reddy, K.; Venkateswarlu, M.; Venkanna, P. Synth Commun 2013, 43, 2672.
26. (a) Ramesh, K.; Shylaja, S.; Rajanna, K. C.; Giridhar Reddy, P.; Saiprakash, P. K. Adv Phys Chem 2013, 146585; (b) Int J Chem Kinet 2014, 46, 126.
27. (a) Glasstone, S.; Laidier, K. J.; Eyring, H.; Theory of Rate Processes; McGraw Hill : New York, 1961; (b) Laidler, K. J. Chemical Kinetics; Pearson Education: Singapore, 2004.
28. Christian, R.; Solvents and Solvent Effects in Organic Chemistry; Wiley-VCH: Weinheim, Germany, 2003.
29. Robinson, R. A.; Stokes, R. H. Electrolyte Solutions; Butterworths Scientific : London, 1955.
30. Brown, D. A.; Hudson, R. F. J Chem Soc 1953, 883.
31. (a) Amis, E. S. Solvent Effects on Reaction Rates and Mechanisms; Academic Press: London, 1964; (b) Kirkwood, J. G. J Chem Phys 1924, 2, 251.
32. (a) Ingold, C. K. Structure and Mechanism in Organic Chemistry; Bell: London, 1953; (b) Hughes, E. D.; Ingold, C. K. J Chem Soc 1935, 244.
33. Kirkwood, J. G.; Grunwald, E.; Winstein, S. J Am Chem Soc 1948, 70, 846.
34. Shorter, J. Correlation Analysis in Organic Chemistry: Introduction to Linear Free-energy Relationships; Clarendon Press, Oxford, UK, 1973; p. 70.
35. Abraham, M. H. Prog Phys Org Chem 1974, 11, 1.
36. Caldin, E. F. Pure Appl Chem 1979, 51, 2067.
37. Reichardt, C. Pure Appl Chem 1982, 54, 1867.
38. Mather, D.; Shorter, J. J Chem Soc, Perkin Trans 1983, 2, 1179.
39. Koppel, I. A.; Palm, V. A. In Advanced Linear Free Energy Relationships; Chapman, N. B.; Shorter, J.; Eds., Plenum Press: London, 1972; Ch. 5.
40. Kamlet, M. J.; Abboud, J. L. M.; Taft, R. W. Prog Phys Org Chem 1981, 13, 485.
41. Abraham, M. H.; Taft, R. W.; Kamlet, M. J. J Org Chem 1981, 46, 3053.
42. Kamlet, M. J.; Abboud, J. L. M.; Abraham, M. H.; Taft, R. W. J Org Chem 1983, 48, 2877.
43. Abraham, M. H. Pure Appl Chem 1985, 57, 1055.
44. Aslan, M. H.; Burden, A. G.; Chapman, N. B.; Shorter, J. J Chem Soc, Perkin Trans 1981, 2, 500.
45. Uscumlic, G. S.; Nikolic, J. B. J Serb Chem Soc 2009, 74, 1335.
46. (a) Hammett, L. P. Physical Organic Chemistry; McGraw-Hill: New York, 1940; (b) Wiberg, K. B. Physical Organic Chemistry; Wiley: New York, 1964.
47. Exner, O. Coll Czech Chem Commun 1955, 1094, 29.
48. (a) Petersen, J. R. C J Org Chem 1964, 29, 3133; (b) Liu, L.; Guo, Q. X. Chem Rev 2001, 101, 673–693; (c) Cornish-Bowden, A. J Biosci 2002, 27, 121–126.
49. (a) Taft, R. W. J Am Chem Soc 1952, 74, 2729; J. Am. Chem. Soc. 1952, 74, 3120; J. Am. Chem. Soc. 1953, 75, 4538; (b) Eric Anslyn, E.; Dougherty, D. A. Modern Physical Organic Chemistry; University Science Books, Sausalito, California. 2006; p. 455.
50. Taft, R. W.; Charton, M. Electrical Effect Substituent Constants for Correlation Analysis; Wiley: New York, 1981; Ch. 3.